

Preprint Notice:

© 2020 IEEE. Personal use of this material is permitted. Permission from IEEE must be obtained for all other uses, in any current or future media, including reprinting/republishing this material for advertising or promotional purposes, creating new collective works, for resale or redistribution to servers or lists, or reuse of any copyrighted component of this work in other works.

arXiv:2009.12703v1 [cs.LG] 26 Sep 2020

An Adaptive EM Accelerator for Unsupervised Learning of Gaussian Mixture Models

Truong Nguyen, Guangye Chen, and Luis Chacón

Abstract

We propose an Anderson Acceleration (AA) scheme for the *adaptive* Expectation-Maximization (EM) algorithm for unsupervised learning a finite mixture model from multivariate data (Figueiredo and Jain 2002). The proposed algorithm is able to determine the optimal number of mixture components autonomously, and converges to the optimal solution much faster than its non-accelerated version. The success of the AA-based algorithm stems from several developments rather than a single breakthrough (and without these, our tests demonstrate that AA fails catastrophically). To begin, we ensure the monotonicity of the likelihood function (a the key feature of the standard EM algorithm) with a recently proposed monotonicity-control algorithm (Henderson and Varahdan 2019), enhanced by a novel monotonicity test with little overhead. We propose nimble strategies for AA to preserve the positive definiteness of the Gaussian weights and covariance matrices strictly, and to conserve up to the second moments of the observed data set exactly. Finally, we employ a K-means clustering algorithm using the gap statistic to avoid excessively overestimating the initial number of components, thereby maximizing performance. We demonstrate the accuracy and efficiency of the algorithm with several synthetic data sets that are mixtures of Gaussians distributions of known number of components, as well as data sets generated from particle-in-cell simulations. Our numerical results demonstrate speed-ups with respect to non-accelerated EM of up to 60 \times when the exact number of mixture components is known, and between a few and more than an order of magnitude with component adaptivity.

Index Terms

unsupervised machine learning, Gaussian mixture model, maximum likelihood estimation, adaptive Expectation-Maximization, Anderson acceleration, monotonicity control, K-means, the gap statistic.

1 INTRODUCTION

THE Gaussian mixture model (GMM) is a probabilistic model that assumes all the observed data points are generated from a mixture of a finite number of Gaussian (normal) distributions [1]–[4]. It has wide applications in pattern recognition and unsupervised machine learning [5], [6], big data analytics [7]–[10], and image segmentation and denoising [11]–[15], as well as recent applications in applied and computational physics, e.g., gas kinetic [16] and plasma kinetic algorithms [17], [18]. Some other applications of GMM can be found in [19]–[22]. Of interest here is a parametric probability density function family of the form $f(\mathbf{x}; \boldsymbol{\theta}) = \sum_{k=1}^K \omega_k G_k(\mathbf{x}; \boldsymbol{\theta}_k)$, where G_k is a Gaussian distribution parameterized by $\boldsymbol{\theta}_k$, ω_k is the a positive weight under the constraint of $\sum_{k=1}^K \omega_k = 1$, and K is the total number of Gaussian components. A common iterative approach to estimate the parameters of the Gaussian distributions in GMM is the Expectation-Maximization (EM) algorithm, which is based on the maximum likelihood principle [2], [23]–[25]. EM is well known for its robustness, as it is guaranteed to converge monotonically to a local maximum. The standard EM algorithm for GMM (EM-GMM) is conceptually simple and easy to implement. However, the performance is highly dependent on the initial guess of the Gaussian parameters and the separation of the Gaussian components (convergence can be very slow when Gaussian components are not well separated). A further difficulty is that the maximum likelihood principle alone cannot determine the number of components [1], [26]. The number of Gaussian components is usually unknown in practice, which makes the proper choice of the number of Gaussian components crucial for the optimal performance of EM-GMM. Choosing too many components would result in overfitting the data set, and potentially worsening the convergence rate of EM-GMM. Alternatively, choosing too few components could result in under-fitting, leading to model predictions that may miss important structures of the data.

To resolve the number of components issue in GMM, a recent and well adopted *adaptive* EM algorithm was proposed [27], [28] that can automatically converge on the optimal number of Gaussian components. By employing a “minimum-message-length (MML)” Bayesian information criterion [29], [30], the method allows users to start with a relatively

- Truong Nguyen is with the Applied Mathematics and Plasma Physics Group, Theoretical Division, Los Alamos National Laboratory, NM 87545, USA, e-mail: tbnnguyen@lanl.gov.
- Guangye Chen is with the Applied Mathematics and Plasma Physics Group, Theoretical Division, Los Alamos National Laboratory, NM 87545, USA, e-mail: gchen@lanl.gov.
- Luis Chacón is with the Applied Mathematics and Plasma Physics Group, Theoretical Division, Los Alamos National Laboratory, NM 87545, USA, e-mail: chacon@lanl.gov.

large number of Gaussian components and gradually converge to the optimal number of groups during EM iterative procedure. Adaptive EM introduces a modified M-step for the Gaussian weights capable of eliminating unimportant components, which is only a simple extension of standard EM-GMM and makes it attractive for practitioners when compared to other methods (e.g., variational Bayesian model [31], and those reviewed in Ref. [26]). Several drawbacks of standard EM, such as sensitivity to initialization, and possible convergence to singular solutions, are also largely avoided [27], [28]. However, the slow convergence problems of standard EM were left unaddressed.

Many methods have been proposed to date to accelerate the convergence rate of standard (*non-adaptive*) EM [25], [32], which may be roughly categorized into EM extension algorithms and gradient-based algorithms. The algorithms in the first category are mainly developed within the EM framework based on statistical considerations, which include ECM [33], ECME [34], SAGE [35], AECM [36], PX-EM [37], and CEMM [38], etc. We note that Figueiredo and Jain's original paper for adaptive EM-GMM employed CEMM, but mainly for the purpose of avoiding elimination of all Gaussian components at the beginning of the iteration in some situations [28]. Algorithms in the second category treat standard EM as a fixed-point iteration map, and seek accelerations using various gradient-based methods, including Aitken-Steffensen-type [23], [39]–[42], conjugate gradient (CG) [43]–[45], quasi-Newton (QN) [46]–[49] and Newton-Raphson [50], [51] methods, etc. In the context of the GMM density estimation, the Newton-Raphson method requires computation of the second derivative of the log-likelihood function (i.e., the Hessian matrix [2]), which is considered too complicated to be practical, especially when compared to standard EM. QN and CG methods avoid the difficulty by using approximations that involve only the first derivatives of the log-likelihood function (i.e., the score function [2]), which are much easier to obtain, and still often gain much acceleration over the standard EM when it is very slow. However, one common feature for many gradient-based EM-accelerators is that they require line-searching and careful monitoring or safeguards, a consequence of the lack of automatic monotone convergence of the likelihood function. The line-search step (e.g., needed in Refs. [43], [44], [46], [47], [49]) determines the step-size in some gradient direction in order to make progress in increasing the likelihood function. This often requires multiple likelihood function evaluations, which is one of the most expensive operations in EM-GMM due to the need to evaluate multiple exponential functions on the sample data. The situation is similar for other strategies such as globalization [41], algorithm restart [42], or monitoring of the progress [49]. The need for many additional likelihood function evaluations can offset much (or even all) of the algorithmic acceleration afforded by these solver strategies, leading to virtually no wall-clock-time advantage.

In this study, we explore acceleration of EM-GMM using Anderson Acceleration (AA) [52], which can be viewed as a variant of QN [53]. We note that AA has been explored before for EM-GMM [54], [55]. In Ref. [54], a reduced mixture problem (i.e., estimating only the means of a three-component univariate Gaussian mixture) was successfully accelerated by AA. Later, Ref. [55] successfully extended the method to two-component multivariate Gaussian mixtures, suggesting potential for AA as an EM-accelerator for GMM. However, both studies assumed a known number of mixture components, and both employed a large number of samples in their tests (10^5 in Ref. [54] and 10^6 in Ref. [55]), presumably robustifying the AA iterations. For smaller and more realistic data sets and more complicated applications, as in some of our tests, the AA implementation in Refs. [54], [55] may break positiveness of Gaussian parameters and may converge to sub-optimal solutions [48] and even fail catastrophically (as we will show). To remedy those drawbacks, we will employ a restarted/regularized version of AA to accelerate *adaptive* EM while monitoring the monotonicity of the likelihood function (a critical step [48]), which has not previously been tested with GMM. In fact, to the best of our knowledge, no gradient-based EM accelerators have been applied to the adaptive EM-GMM algorithm.

The success of our proposed algorithm stems from various ingredients. Firstly, we improve the monotonicity control step proposed in Ref. [48] with a new, very low overhead monotonicity test. Secondly, we ensure that the algorithm preserves positive-definiteness of Gaussian weights and covariance matrices, and conserves up to second moments of the observed data set exactly, just as in a standard EM. Lastly, it is well known that choosing the initial number of Gaussians well can significantly affect the performance of adaptive EM. To obtain a good estimate for the initial number of components, we complement our method with a reliable initialization routine using K-means clustering with the gap statistic [56]. As a result, our AA-based algorithm delivers significant efficiency gains versus the non-accelerated EM while converging to the same (optimal) solution.

The rest of the paper is organized as follows. Section 2 introduces the basic concepts of both standard and adaptive EM-GMM. Section 3 briefly summarizes a recent attempt at EM acceleration, the exact-line-search (ELS) EM (which we will use as a benchmark for performance). We then present an overview of AA, its challenges of aggressive application to EM-GMM, and strategies to address these challenges proposed in the literature. Section 4 proposes our solution for accelerating adaptive EM with monotonicity control for the likelihood function. Key elements include the design of an efficient approach for monotonicity control in AA, the use of a regularization term [48] to combine the robustness of EM and local convergence speed of AA, and the careful selection of the initial number of Gaussian components using K-means clustering based on the gap statistic approach [56]. Also described are our solutions for strict moment conservation and preservation of positive-definiteness of Gaussian weights and covariance matrices. Section 5 demonstrates the fidelity and efficiency of the proposed acceleration scheme over its non-accelerated counterpart for several synthetic data sets, as well as real data sets generated from particle-in-cell simulations [17], where we demonstrate significant algorithmic and wall-clock-time speed-ups. Finally, we conclude in Section 6.

2 THE EXPECTATION MAXIMIZATION (EM) ALGORITHM FOR GAUSSIAN MIXTURES (EM-GMM)

A Gaussian mixture (GM) of K components is defined to be a convex combination of K Gaussian distributions G_k , $k = 1, \dots, K$ of the following form

$$f(\mathbf{x}) = \sum_{k=1}^K \omega_k G_k(\mathbf{x}; \boldsymbol{\mu}_k, \boldsymbol{\Sigma}_k), \quad (1)$$

where ω_k , $\boldsymbol{\mu}_k$, $\boldsymbol{\Sigma}_k$ are the weight, mean and covariance matrix, respectively, of the k th Gaussian in the mixture. Note that $\omega_k \geq 0$, and $\boldsymbol{\Sigma}_k$ are symmetric-positive-definite matrices. The Gaussian distribution G_k is defined as

$$G_k(\mathbf{x}; \boldsymbol{\mu}_k, \boldsymbol{\Sigma}_k) = \frac{1}{\sqrt{(2\pi)^D |\boldsymbol{\Sigma}_k|}} e^{-\frac{1}{2}(\mathbf{x}-\boldsymbol{\mu}_k)^T \boldsymbol{\Sigma}_k^{-1}(\mathbf{x}-\boldsymbol{\mu}_k)} \quad (2)$$

where both \mathbf{x} and $\boldsymbol{\mu}$ are D -dimensional column vectors, the superscript T denotes transpose, and $|\boldsymbol{\Sigma}_k|$ is the determinant of the covariance matrix.

2.1 The standard EM-GMM algorithm

The goal is to find the Gaussian parameters $\boldsymbol{\theta} = (\boldsymbol{\theta}_1, \dots, \boldsymbol{\theta}_K)$ where $\boldsymbol{\theta}_k = (\omega_k, \boldsymbol{\mu}_k, \boldsymbol{\Sigma}_k)$ for $k = 1, \dots, K$ that maximize the log-likelihood of the Gaussian mixture model [57]. The log-likelihood is written as

$$\begin{aligned} \mathcal{L}(\boldsymbol{\theta}) &= \ln \left(\prod_{j=1}^N \left[f(\mathbf{x}_j) \right]^{\zeta_j} \right) + \eta \left(\sum_{k=1}^K \omega_k - 1 \right) \\ &= \sum_{j=1}^N \zeta_j \ln \left(\sum_{k=1}^K \omega_k G_k(\mathbf{x}_j; \boldsymbol{\mu}_k, \boldsymbol{\Sigma}_k) \right) + \eta \left(\sum_{k=1}^K \omega_k - 1 \right), \end{aligned} \quad (3)$$

for N independent samples $\mathbf{X} = (\mathbf{x}_1, \dots, \mathbf{x}_N)$ (presumably) drawn from $f(\mathbf{x})$, with each sample \mathbf{x}_j having a weight ζ_j . Here, $\eta \left(\sum_{k=1}^K \omega_k - 1 \right)$ is the Lagrange-multiplier term that enforces the normalization constraint $\sum_{k=1}^K \omega_k = 1$, i.e., $f(\mathbf{x})$ is normalized to unity. We assume that $\sum_{j=1}^N \zeta_j = N$, and the sample weights ζ_j , $j = 1, \dots, N$ account for the cases with non-identical samples [58].

In order to maximize the log-likelihood function $\mathcal{L}(\boldsymbol{\theta})$, we solve the following score equations:

$$\frac{\partial \mathcal{L}(\boldsymbol{\theta})}{\partial \boldsymbol{\theta}} = 0, \text{ and } \frac{\partial \mathcal{L}(\boldsymbol{\theta})}{\partial \eta} = 0. \quad (4)$$

We obtain (see Ref. [5] and Appendix A):

$$\boldsymbol{\mu}_k = \frac{1}{N_k} \sum_{j=1}^N r_{jk} \mathbf{x}_j, \quad (5)$$

$$\boldsymbol{\Sigma}_k = \frac{1}{N_k} \sum_{j=1}^N r_{jk} (\mathbf{x}_j - \boldsymbol{\mu}_k)(\mathbf{x}_j - \boldsymbol{\mu}_k)^T, \quad (6)$$

$$\omega_k = \frac{N_k}{N}, \quad (7)$$

where r_{jk} is the responsibility value of point \mathbf{x}_j within the k th Gaussian, and is defined as:

$$r_{jk} = \frac{\zeta_j \omega_k G_k(\mathbf{x}_j; \boldsymbol{\mu}_k, \boldsymbol{\Sigma}_k)}{\sum_{l=1}^K \omega_l G_l(\mathbf{x}_j; \boldsymbol{\mu}_l, \boldsymbol{\Sigma}_l)}, \quad (8)$$

with $N_k = \sum_{j=1}^N r_{jk}$ and $\zeta_j = \sum_{k=1}^K r_{jk}$.

EM-GMM is an iterative procedure to find the solution to (5), (6) and (7), and can be done in the following distinct steps until convergence:

- Expectation-step: Evaluate the responsibilities r_{jk} for $j = 1, \dots, N$ and $k = 1, \dots, K$ using (8).
- Maximization-step: Update the Gaussian parameters for $k = 1, \dots, K$ using (5), (6) and (7).

Convergence of the algorithm is assessed by monitoring the log-likelihood function (3). We note that several quantities used in the computation of responsibilities for $\theta^{(it)}$, $r_{jk}^{(it)}$ ($\theta^{(it)}$), can be re-used in the evaluation of $\mathcal{L}(\theta^{(it)})$ for efficiency. We remark that each EM iteration ensures the monotonic increase of the likelihood function during the iteration [23], and conserves up to the second moments of the data set [17], [59].

2.2 The adaptive EM-GMM algorithm

In practice, the number of Gaussian components in the Gaussian mixture is often unknown. Therefore, a way to select the proper number of mixture components is needed. Component adaptivity can be accomplished by employing the minimum message length (MML) criterion [17], [27]–[30], [60] to penalize the log-likelihood function. Instead of using (3) for the log-likelihood, we use the following penalized log-likelihood function:

$$\begin{aligned} \mathcal{P}\mathcal{L}(\boldsymbol{\theta}) = & \sum_{j=1}^N \zeta_j \ln \left(\sum_{k=1}^K \omega_k G_k(\mathbf{x}; \boldsymbol{\mu}_k, \boldsymbol{\Sigma}_k) \right) + \eta \left(\sum_{k=1}^K \omega_k - 1 \right) \\ & - \frac{d}{2} \ln(N) - \frac{T}{2} \sum_{k=1}^K \ln(\omega_k), \end{aligned} \quad (9)$$

where d is the total number of parameters in the Gaussian mixture and $T = \frac{D(D+3)}{2}$. For a detailed derivation of (9), we refer the reader to Ref. [17]. The last two terms in (9) are the penalization terms, and they play an important role in determining the optimal number of components by removing unnecessary Gaussian components in order to avoid over-fitting the data.

In order to maximize the penalized log-likelihood function (9), the same approach as described in Section 2.1 results in the same formulas for updating the Gaussians' means $\boldsymbol{\mu}_k$ and covariance matrices $\boldsymbol{\Sigma}_k$ in the M-step, i.e., (5) and (6), respectively. However, due to the presence of the penalization terms, the equation for the Gaussians' weights is modified as (see Appendix A):

$$\omega_k = \frac{N_k - \frac{T}{2}}{N - \frac{TK}{2}}, \quad (10)$$

provided that $N_k > T/2$. If $N_k < T/2$, $\omega_k < 0$, indicating that the k th Gaussian should be killed. Also, (10) advises that one should start with more Gaussian components than the exact number of Gaussian components in the GMM [61].

Putting things together, assuming K components at each iteration of adaptive EM-GMM, we do the following:

- 1) Evaluate the responsibilities r_{jk} using (8).
- 2) Compute $\omega_k^{(*)} = \max\left(\frac{N_k - T/2}{N - TK/2}, 0\right)$.
- 3) If $\omega_k^{(*)} = 0$ then kill the k th Gaussian: set $\boldsymbol{\mu}_k = 0$, $\boldsymbol{\Sigma}_k = 0$ and $K = K - 1$. Otherwise, update the mean and covariance matrix of the k th Gaussian using (5) and (6), respectively.
- 4) Re-normalize the Gaussian weights: $\omega_k = \omega_k^{(*)} / (\sum_{k=1}^K \omega_k^{(*)})$.
- 5) Check for convergence by monitoring the penalized log-likelihood function (9).

Steps 1 to 5 are repeated until convergence. We refer to Step 1 as the E-step and Steps 2-4 as the M-step. In practice, we can perform the iterations in a simultaneous approach or a component-wise approach [38]. In the simultaneous EM, we perform the E-step for all available Gaussian components in the mixture, then update their parameters in the M-step. In the component-wise EM, we perform the E-M steps for one Gaussian component and then move on to the next one until we reach the final component in the mixture. The simultaneous approach is faster but the algorithm could possibly kill all Gaussians at once in some situations (e.g., when the starting number of components, K_{init} , is much larger than the model's exact number of components, K_{model}) [28]. The component-wise approach is slower (because it requires updating the Gaussian mixture's probability density function once a component is updated) but it can prevent such a problem [28]. For efficiency, here we follow the simultaneous approach while relying on an extended form of K-means clustering [56], [62]–[66] to provide a good initial guess for the number of components. This will be discussed later in this study.

We note that both the accelerated and non-accelerated versions of the adaptive EM-GMM iteration do not conserve the moments of the observed data set due to the presence of the penalization terms. To recover conservation, we perform a final standard EM-GMM step after convergence [17].

3 NONLINEAR ACCELERATION OF THE EM ALGORITHM

3.1 State of the art in accelerated EM-GMM: Exact Line Search method (ELS-EM)

A recent attempt to accelerate EM-GMM is the so-called exact line search EM (ELS-EM) introduced by Xiang et al. [67]. The strategy of the method is to search for an improved solution, $\boldsymbol{\theta}^{(new)} = (\omega_k^{(new)}, \boldsymbol{\mu}_k^{(new)}, \boldsymbol{\Sigma}_k^{(new)})$, which is along the line joining the current and previous iterates, before updating the Gaussian parameters in the M-step. In particular, we want to find $\boldsymbol{\rho}^{(it)} = (\rho_{\omega_k}, \rho)$, where ρ_{ω_k} is the step size for each Gaussian weight ω_k and ρ is the common step size for all Gaussian means and covariance matrices in GMM [67], such that

$$\begin{aligned} \omega_k^{(new)} &= \omega_k^{(it-1)} + \rho_{\omega_k} (\omega_k^{(it)} - \omega_k^{(it-1)}), \\ \boldsymbol{\mu}_k^{(new)} &= \boldsymbol{\mu}_k^{(it-1)} + \rho (\boldsymbol{\mu}_k^{(it)} - \boldsymbol{\mu}_k^{(it-1)}), \\ \boldsymbol{\Sigma}_k^{(new)} &= \boldsymbol{\Sigma}_k^{(it-1)} + \rho (\boldsymbol{\Sigma}_k^{(it)} - \boldsymbol{\Sigma}_k^{(it-1)}), \end{aligned} \quad (11)$$

maximizes the log-likelihood. Here, the superscripts indicate solutions at current (it)th and previous ($it-1$)th iteration, respectively. Details for the computation of the step sizes $\rho^{(it)}$ can be found in Ref. [67]. If $\mathcal{L}(\boldsymbol{\theta}^{(new)}) > \mathcal{L}(\boldsymbol{\theta}^{(it)})$, we use $\boldsymbol{\theta}^{(new)}$ to update the Gaussian parameters in M-step instead of using $\boldsymbol{\theta}^{(it)}$. The sketch for one iteration of ELS-EM [67] is as follows:

- 1) E-step: Evaluate the responsibilities $r_{jk}^{(it)}(\boldsymbol{\theta}^{(it)})$ using (8).
- 2) ELS-step: Compute the solution $\boldsymbol{\theta}^{(new)}$ using (11). If $\mathcal{L}(\boldsymbol{\theta}^{(new)}) > \mathcal{L}(\boldsymbol{\theta}^{(it)})$, evaluate $r_{jk}^{(new)}(\boldsymbol{\theta}^{(new)})$ and set $r_{jk}^{(it)} = r_{jk}^{(new)}$, else, keep $r_{jk}^{(it)}$ from the E-step.
- 3) M-step: Update Gaussian parameters $\boldsymbol{\theta}^{(it+1)}$ using $r_{jk}^{(it)}$.

It was pointed out in Ref. [67] that the cost of the ELS-step is the same as the cost of the E-step, since it needs an additional evaluation of the log-likelihood function and the re-evaluation of responsibilities r_{jk} when the new solution $\boldsymbol{\theta}^{(new)}$ is better. This makes one iteration of ELS-EM about two times more expensive than one EM iteration. We have implemented ELS for standard (non-adaptive) EM-GMM, and we have confirmed that this is the case (as we will show). Moreover, we have found a reduction in iteration count of only $\sim 2 - 2.5\times$ with ELS-EM for our synthetic data sets, resulting in almost no wall-clock-time speed up. This is in contrast with our proposed algorithm, described in the next section, where we demonstrate wall-clock-time speed-ups up to $\sim 60\times$ for the same data sets.

3.2 Anderson acceleration of EM

AA is a common accelerator for nonlinear Picard iterative procedures [52], [54], [68]. EM-GMM is indeed a Picard iteration, which can show slow convergence especially in the case where the Gaussians in the mixture are highly overlapping. Therefore, in principle, it can be accelerated by Anderson acceleration. A direct application of AA for EM (AAEM), taken from [54], is given in Algorithm 1. In the algorithm, $\mathbf{G}(\boldsymbol{\theta})$ is one step of either standard or adaptive EM-GMM.

Algorithm 1 Anderson accelerated EM algorithm (AAEM)

Given initial solution, $\boldsymbol{\theta}^{(0)}$ and maximum number of residuals, $m_{AA} \geq 1$.

Evaluate $\boldsymbol{\theta}^{(1)} = \mathbf{G}(\boldsymbol{\theta}^{(0)})$.

Do $it = 1, 2, \dots$ until converged:

- 1) Set the number of residuals in AA, $m = \min(it, m_{AA})$.
- 2) Set $\mathbf{F}_{it} = (\mathbf{f}_{it-m}, \dots, \mathbf{f}_{it})$ where $\mathbf{f}_i = \mathbf{G}(\boldsymbol{\theta}^{(i)}) - \boldsymbol{\theta}^{(i)}$.
- 3) Solve for $\boldsymbol{\alpha}^{(it)}$ such that

$$\boldsymbol{\alpha}^{(it)} = \operatorname{argmin}_{\boldsymbol{\alpha}} \|\mathbf{F}_{it}\boldsymbol{\alpha}\| \text{ subject to } \sum_{i=0}^m \alpha_i = 1. \quad (12)$$

- 4) $\boldsymbol{\theta}^{(it+1)} = \sum_{i=0}^m \alpha_i^{(it)} \mathbf{G}(\boldsymbol{\theta}^{(it-m+i)})$.

- 5) Check for convergence by monitoring log-likelihood (use (3) for standard EM or (9) for adaptive EM).
-

Unfortunately, several problems arise when one naively applies AA to EM-GMM. Firstly, for both standard and adaptive cases, our numerical experiments show that AAEM only conserves the zeroth moment of the given data set. Secondly, the positive-definiteness property of the Gaussian weights and covariance matrices is not ensured with standard AA since the Anderson iterate is expressed as a non-convex linear combination of positive-definite solutions [69], [70] (i.e., some of the AA coefficients α_i in (12) can be negative). Thirdly, the monotonicity of the log-likelihood function is not ensured. From our numerical results, we often see that the log-likelihood of the Anderson solution is less than the log-likelihood of the current EM iterate, i.e., $\mathcal{L}(\boldsymbol{\theta}^{(AA)}) < \mathcal{L}(\boldsymbol{\theta}^{(it)})$ in the standard case, or $\mathcal{P}\mathcal{L}(\boldsymbol{\theta}^{(AA)}) < \mathcal{P}\mathcal{L}(\boldsymbol{\theta}^{(it)})$ in the adaptive case. Fourthly, in adaptive EM, since the exact number of Gaussian components is unknown, we often start with a larger number of components than needed for a given data set. In this case, when applying AA for adaptive EM-GMM, we observe that the method does not produce the right number of Gaussian components and converges to a non-optimal solution. In some situations, the convergence rate of adaptive AAEM is observed to be slower than that of the adaptive non-accelerated EM, as we will demonstrate in a later section.

We have explored various solutions proposed in the literature to address these issues, with varied success. To preserve up to second moments at every iteration, we considered accelerating Gaussian moments $\mathbf{M}_k = \omega_k(1, \boldsymbol{\mu}_k, \boldsymbol{\Sigma}_k + \boldsymbol{\mu}_k \boldsymbol{\mu}_k^T)$ instead of the Gaussian parameters $\boldsymbol{\theta}_k = (\omega_k, \boldsymbol{\mu}_k, \boldsymbol{\Sigma}_k)$. We find that this approach conserves up to second moments in the non-adaptive case with fixed number of Gaussian components, but not in the adaptive case because of the renormalization of the Gaussian weights in the M-step. In addition, the moment-acceleration strategy may break the positive-definiteness of $\boldsymbol{\Sigma}_k$ when computed from the second moment matrix $\mathcal{M}_{k,2}$. To address the positive-definiteness of Gaussian weights and covariance matrices, we employed the AA globalization technique proposed in [70], i.e., an additional constraint for the positivity of the AA coefficients is added to the least square problem (12) as follows

$$\begin{aligned} & \text{Find } \boldsymbol{\alpha}^{(it)} \text{ s.t. } \boldsymbol{\alpha}^{(it)} = \operatorname{argmin}_{\boldsymbol{\alpha}} \|\mathbf{F}_{it} \boldsymbol{\alpha}\| \\ & \text{subject to } \sum_{i=0}^m \alpha_i = 1 \text{ and } \alpha_i > 0 \quad \forall i, \end{aligned} \quad (13)$$

where m is the number of past residuals in AA at the (it) th iteration. We found from our numerical experiments that this approach significantly slows down the local convergence speed of AA (since it restricts the optimization domain), and that, at a later phase in the AAEM iteration, it frequently defaults back to EM, i.e., it returns $\alpha_m = 1$ and $\alpha_0 = \dots = \alpha_{m-1} = 0$.

To address successfully the AAEM problem of local convergence to a non-optimal solution, we follow the AA regularization approach proposed by Henderson et al. [48]. Specifically, the constrained least-squares problem (12) can be reformulated as an unconstrained least-squares problem to which a regularization term $\lambda \mathbf{I}_{m \times m}$ is added as follows (see [48], [54]):

$$\text{At } (it)\text{th iteration, find } \boldsymbol{\gamma}^{(it)} \text{ s.t. } (\mathcal{F}_{it}^T \mathcal{F}_{it} + \lambda \mathbf{I}) \boldsymbol{\gamma}^{(it)} = \mathbf{F}_{it}^T \mathbf{f}_{it}, \quad (14)$$

where $\mathcal{F}_{it} = (\Delta \mathbf{f}_{it-m}, \dots, \Delta \mathbf{f}_{it-1})$, $\Delta \mathbf{f}_i = \mathbf{f}_{i+1} - \mathbf{f}_i$ and $\mathbf{f}_i = \mathbf{G}(\boldsymbol{\theta}^{(i)}) - \boldsymbol{\theta}^{(i)}$. As remarked in Ref. [54], there exists a one-to-one correspondence between the coefficients $\boldsymbol{\alpha}^{(it)}$ given by (12) and the coefficients $\boldsymbol{\gamma}^{(it)}$ given by (14) when $\lambda = 0$, that is:

$$\begin{aligned} \alpha_0^{(it)} &= \gamma_0^{(it)}, \quad \alpha_i^{(it)} = \gamma_i^{(it)} - \gamma_{i-1}^{(it)} \text{ for } i = 1, \dots, m-1, \\ \alpha_m^{(it)} &= 1 - \gamma_{m-1}^{(it)}. \end{aligned}$$

In this case, at the (it) th iteration, the updated Anderson iterate can be written as

$$\boldsymbol{\theta}^{(it+1)} = \mathbf{G}(\boldsymbol{\theta}^{(it)}) - \sum_{i=0}^{m-1} \gamma_i^{(it)} [\mathbf{G}(\boldsymbol{\theta}^{(it-m+i+1)}) - \mathbf{G}(\boldsymbol{\theta}^{(it-m+i)})]. \quad (15)$$

According to Henderson et al. [48], the use of the regularization term $\lambda \mathbf{I}$ helps combine the convergence robustness of EM and the local convergence speed of AA. One can see that if $\lambda = 0$, we recover AA, and if $\lambda \gg 1$, we recover EM. We refer to Ref. [48] for the strategy of computing λ at each EM iteration, which we follow strictly. This approach, together with a novel, very efficient monotonicity-control implementation for the log-likelihood function (discussed in the next section) results in an algorithm that captures the right number of components and quickly converges to the right solution nearly without run-time penalty.

4 THE ADAPTIVE ACCELERATED-MONOTONICITY-PRESERVING EXPECTATION-MAXIMIZATION (A-AMEM) ALGORITHM

The main goal of this paper is to make the adaptive EM (A-EM) algorithm faster. To this end, we apply an Anderson acceleration to A-EM while maintaining key features of both adaptive and standard EM such as component adaptivity, conservation of up to second moments, preservation of positive-definiteness of Gaussian weights and covariance matrices, and monotonicity preservation of the log-likelihood function during the iteration. The adaptive, accelerated, monotonicity-preserving EM (A-AMEM) algorithm for GMM is outlined in Section 4.1, with the initialization and implementation details discussed in Sections 4.2 and 4.3, respectively.

4.1 The main A-AMEM algorithm

The accelerated algorithm for the adaptive EM-GMM iteration is detailed in Algorithm 2. We implement the regularization term [48] and employ the AA periodical restart [48], [68], [71] to address some of the pitfalls of a naive AAEM implementation for adaptive GMM. In Algorithm 2, $\mathbf{G}(\boldsymbol{\theta})$ represents the fixed-point EM step of A-EM, λ is the regularization factor and ϵ is the log-likelihood controlling parameter. Details on Algorithm 2 and further discussions for the values of λ and ϵ are given next.

4.2 Initialization of A-AMEM

We use K-means clustering for Gaussian initialization. The initial centroids of the clusters in each K-means call are selected from the data points with an improved seeding technique [72]. To obtain the best guess for the number of components, we employ the gap statistic (GS) method [56], using the so-called the gap statistic value (GSV). (We have also explored other K-means techniques [62], [63], [65], [66] and we will discuss them in Section 5.9.) The GSV associated to K clusters is defined as (cf. [56]):

$$GSV(K) = E^* [\ln(SSE_K)] - \ln(SSE_K). \quad (16)$$

In (16), E^* denotes the expectation under a sample from the reference distribution, and SSE_K is given as:

$$SSE_K = \sum_{k=1}^K \sum_{\mathbf{x}_i \in \mathcal{C}_k} \zeta_i |\mathbf{x}_i - \mathbf{c}_k|^2, \quad (17)$$

Algorithm 2 Adaptive accelerated-monotonicity EM (A-AMEM) algorithm

Given

- m_{AA} , the maximum number of residuals for AA.
- K_{init} , the initial number of components to be used.

Initialization: Perform K-means clustering algorithm with K_{init} clusters (multiple times and select the best run) to obtain the initial solutions $\theta^{(0)}$.

The adaptive AMEM: Do $it = 0, 1, 2, \dots$ until converged:

- 1) Perform **EM** step: $\theta^{(it+1)} = \mathbf{G}(\theta^{(it)})$. During this step, Gaussian(s) may be killed. Restart AA if a Gaussian component is eliminated.
- 2) Apply **regularized AA**:
Solve the least square problem (14) for $\gamma^{(it)}$.
Compute the Anderson iterate, $\theta^{(AA)}$, using (15). If any Gaussian weight becomes negative, then use EM solution and continue to the next iteration.
Else, go to Step 3.
- 3) **Monotonicity control**:
If $\mathcal{PL}(\theta^{(AA)}) - \mathcal{PL}(\theta^{(it)}) > -\epsilon$ then set $\theta^{(it+1)} = \theta^{(AA)}$,
Else, use EM solution.
- 4) **Restart AA** if number of residual vectors reaches m_{AA} .
- 5) Check for convergence by monitoring the penalized log-likelihood given by (9).

Conservation of moments: Perform one final standard EM step after convergence.

where \mathcal{C}_k is the k th cluster and ζ_i is the weight for point $\mathbf{x}_i \in \mathcal{C}_k$.

The computation of the expectation in $GSV(K)$ is done with Monte-Carlo from reference data sets (see Ref. [56]). We have found that generating the reference sets from a uniform distribution over a box aligned with the principal components of the observed sample [56] (which is the one we use in our numerical simulations in Section 5.9), or from a unit normal distribution with parameters taken to be the sample's mean and covariance matrix yields reliable results for our data sets.

The optimal number of clusters K_{opt} is found from the following condition:

$$K_{opt} = \text{smallest } K \text{ s.t. } GSV(K) > GSV(K+1) + \tau \times s_{K+1} \quad (18)$$

for $K = K_{min}, \dots, K_{max}$. In (18), s_K is the standard deviation term which accounts for the Monte Carlo simulation error in evaluating $GSV(K)$, and τ is user-input factor that represents the amount of standard deviation used. We refer the reader to Ref. [56] for more details on the evaluation of $GSV(K)$ and s_K . In our application, choosing $\tau = 0$ or 1 in (18) instead of $\tau = -1$ as in Ref. [56] helps avoid possible under-estimation of number of clusters by the GS method. Although it may potentially over-estimate the number of clusters by a few in some cases, this is acceptable in our application since, for robustness, A-AMEM should begin with more components than the expected number. Once the optimal number of clusters is obtained, we set the initial number of clusters as $K = K_{opt} + K_{adjust}$ for some $K_{adjust} > 0$, to further avoid under-estimation of the model. We then repeat K-means with K clusters multiple times and the centroids associated with the best trial are selected. The best trial is the one that yields the smallest inertia (SSE) value. The initial Gaussian means $\mu_k^{(0)}$, $k = 1, \dots, K$ are assigned from the clusters' centroids of the best run. The initial Gaussians weights are computed from the K-means best run as:

$$\omega_k^{(0)} = \frac{n_k}{N}$$

where $n_k = \sum_{i \in \mathcal{C}_k} \zeta_i$ is the total weight of points that belong to the k th cluster and N is the total number of observed points in the data set. The initial Gaussians' covariance matrices can be assigned to the clusters' so-called within-covariances, which are evaluated as:

$$\Sigma_k^{(0)} = \frac{1}{n_k} \sum_{j=1}^{n_k} \zeta_i (\mathbf{x}_j - \mu_k^{(0)}) (\mathbf{x}_j - \mu_k^{(0)})^T,$$

where $\mathbf{x}_j, j = 1, \dots, n_k$ are the points assigned to the k th cluster at the end of the K-means iteration. In general, the K-means initialization algorithm for EM is quite inexpensive compared to EM, taking a small fraction (5-10%) of the total wall-clock time, and can have a large impact in the efficiency of the overall algorithm.

4.3 Implementation details of A-AMEM

For the adaptive EM algorithms, we follow the steps outlined in Section 2.2 to compute the updated Gaussians' parameters. We remark that the k th Gaussian is removed from the mixture if the updated weight is negative.

Additionally, we perform a restart of AA if a Gaussian component is killed during this step, since the past AA solution history of the removed component is no longer valid.

Once we obtain the updated values for the Gaussian parameters, we solve the unconstrained regularized least-square problem (14), and compute the updated AA solution, $\boldsymbol{\theta}^{(AA)}$, using (15). To ensure positive-definiteness of covariance matrices, we accelerate the entries of the matrices \mathbf{L}_k , $k = 1, \dots, K$ where $\boldsymbol{\Sigma}_k = \mathbf{L}_k \mathbf{L}_k^T$ is the Cholesky decomposition [73] of $\boldsymbol{\Sigma}_k$ for $k = 1, \dots, K$. After the acceleration procedure, the covariance matrices $\boldsymbol{\Sigma}_k$ can be recovered using the lower-triangular matrices \mathbf{L}_k for $k = 1, \dots, K$. As for the Gaussian weights, if AA returns $\omega_l < 0$ for some $l = 1, \dots, K$, then we simply roll back to the EM solution, which is guaranteed to keep Gaussian weights positive and increase the penalized log-likelihood function. We note that the violation of positive-definiteness of the Gaussian weights does not occur frequently during the A-AMEM iteration, about 1%–5% of the time for our synthetic data sets. Hence, the local convergence speed of AA is not much affected by the development of negative weights, and thus the rollback-to-EM strategy seems reasonable.

The monotonicity control step (step 3 in Algorithm 2) is expensive because in principle it requires an additional evaluation of the log-likelihood function (9), which involves loops over all samples and available Gaussian components and expensive logarithmic and exponential evaluations. As a result, one iteration of A-AMEM becomes twice as expensive as one A-EM iteration. To avoid evaluating the penalized log-likelihood function for the AA iterate, $\mathcal{P}\mathcal{L}(\boldsymbol{\theta}^{(AA)})$, in the monotonicity control step, we approximate the computation of $\mathcal{P}\mathcal{L}(\boldsymbol{\theta}^{(AA)}) - \mathcal{P}\mathcal{L}(\boldsymbol{\theta}^{(it)})$ using a first-order Taylor expansion, which relies on the exact evaluation of score functions. We recall that the score function is the derivative of the log-likelihood function with respect to the Gaussian unknowns. In particular, instead of checking

$$\mathcal{P}\mathcal{L}(\boldsymbol{\theta}^{(AA)}) - \mathcal{P}\mathcal{L}(\boldsymbol{\theta}^{(it)}) > -\epsilon, \quad (19)$$

we check

$$\frac{\partial \mathcal{P}\mathcal{L}(\boldsymbol{\theta})}{\partial \boldsymbol{\theta}^{(it)}} \cdot (\boldsymbol{\theta}^{(AA)} - \boldsymbol{\theta}^{(it)}) > -\epsilon, \quad (20)$$

where $\epsilon > 0$ is the monotonicity parameter, and

$$\frac{\partial \mathcal{P}\mathcal{L}(\boldsymbol{\theta})}{\partial \omega_k^{(it)}} = \frac{N_k^{(it)}}{\omega_k^{(it)}} - \frac{T}{2\omega_k^{(it)}} - N + \frac{TK}{2}, \quad (21)$$

$$\frac{\partial \mathcal{P}\mathcal{L}(\boldsymbol{\theta})}{\partial \boldsymbol{\mu}_k^{(it)}} = (\boldsymbol{\Sigma}_k^{(it)})^{-1} \left[\sum_{j=1}^N r_{jk}^{(it)} (\mathbf{x}_j - \boldsymbol{\mu}_k^{(it)}) \right], \quad (22)$$

$$\frac{\partial \mathcal{P}\mathcal{L}(\boldsymbol{\theta})}{\partial \boldsymbol{\Sigma}_k^{(it)}} = (\boldsymbol{\Sigma}_k^{(it)})^{-1} \left\{ \sum_{j=1}^N \frac{r_{jk}^{(it)}}{2} \left[-\boldsymbol{\Sigma}_k^{(it)} + (\mathbf{x}_j - \boldsymbol{\mu}_k^{(it+1)})(\mathbf{x}_j - \boldsymbol{\mu}_k^{(it+1)})^T \right] \right\} (\boldsymbol{\Sigma}_k^{(it)})^{-1}, \quad (23)$$

for $k = 1, \dots, K$. Details on the derivation of (21), (22) and (23) are given in Appendix A. Using (20) is cheap because most quantities in (21), (22) and (23) can be re-used from the adaptive M step in Algorithm 2. Thus, the evaluation complexity for the gradient $\frac{\partial \mathcal{P}\mathcal{L}(\boldsymbol{\theta})}{\partial \boldsymbol{\theta}^{(it)}}$ is only of order $O(KD)$ where D is the dimension of $\boldsymbol{\mu}_k^{(it)}$. This is much more efficient than the direct evaluation of $\mathcal{P}\mathcal{L}(\boldsymbol{\theta}^{(AA)})$, which has computational complexity of $O(NKD)$, where $N \gg 1$ is the number of sample data points. The Taylor expansion approach for approximating $\mathcal{P}\mathcal{L}(\boldsymbol{\theta}^{(AA)}) - \mathcal{P}\mathcal{L}(\boldsymbol{\theta}^{(it)})$ renders the cost of one A-AMEM iteration comparable to one A-EM iteration, and is a key contributor to the efficiency improvement of our implementation. As for the monotonicity parameter ϵ , we find that using values of $\epsilon \in [0.001, 0.01]$ works well for our simulations. Choosing $\epsilon = 0.01$ means that likelihood ratios between current and accelerated solutions are allowed to be no greater than $e^\epsilon \approx 1.01$ [48]. Further discussion about the choice of ϵ can be found in the same reference.

We apply a periodic restart strategy for AA in A-AMEM to help improve the overall robustness of the algorithm, as suggested in [48], [71]. The AA restart solution proposed in [71] kept the last column of \mathcal{F}_{it} . We have tested both resetting all AA residuals to zero and keeping the latest column of \mathcal{F}_{it} , and found that they yield comparable performance for our numerical tests.

Finally, once the algorithm converges to a solution with an optimal number of Gaussian components, we perform one final standard EM iteration (see Section 2.1 and [17]) to recover the conservation up to second moments of the observed data set.

5 NUMERICAL RESULTS

We apply A-AMEM (Algorithm 2) and A-EM to several synthetic GMM data sets and compare the performance and results of the two algorithms. Each synthetic data set is a convex linear combination of $K_{exact} = 3$ Gaussian distributions with different overlap. Each set consists of $N = 1000$ points. The separation between Gaussians can be measured by the Euclidean distances of the Gaussians' means and the Gaussians' shapes, determined by covariance matrices. We generate three synthetic data sets, namely Very Well Separated (VWS), Poorly Separated (PS) and Very Poorly Separated (VPS), with Gaussian means given as follows:

$$\text{VWS: } \boldsymbol{\mu}_1 = \begin{bmatrix} -3 \\ -3 \\ -3 \end{bmatrix}, \boldsymbol{\mu}_2 = \begin{bmatrix} 0 \\ 0 \\ 0 \end{bmatrix}, \boldsymbol{\mu}_3 = \begin{bmatrix} 3 \\ 3 \\ 3 \end{bmatrix},$$

$$\text{PS: } \boldsymbol{\mu}_1 = \begin{bmatrix} -2 \\ -2 \\ -2 \end{bmatrix}, \boldsymbol{\mu}_2 = \begin{bmatrix} 0 \\ 0 \\ 0 \end{bmatrix}, \boldsymbol{\mu}_3 = \begin{bmatrix} 2 \\ 2 \\ 2 \end{bmatrix},$$

$$\text{VPS: } \boldsymbol{\mu}_1 = \begin{bmatrix} -1 \\ -1 \\ -1 \end{bmatrix}, \boldsymbol{\mu}_2 = \begin{bmatrix} 0 \\ 0 \\ 0 \end{bmatrix}, \boldsymbol{\mu}_3 = \begin{bmatrix} 1 \\ 1 \\ 1 \end{bmatrix}.$$

For the Gaussian weights and covariance matrices, we choose:

$$\omega_1 = 0.3, \omega_2 = 0.3, \omega_3 = 0.4,$$

$$\boldsymbol{\Sigma}_1 = \text{diag}(1, 1, 1), \boldsymbol{\Sigma}_2 = 1.5\boldsymbol{\Sigma}_1, \boldsymbol{\Sigma}_3 = 0.75\boldsymbol{\Sigma}_1,$$

for the three manufactured GMM data sets. We also apply Algorithm 2 to real data sets generated from collisionless plasma particle-in-cell (PIC) simulations [17]. These real data sets consist of electrons' velocity points in the three dimensional (3D) velocity space, and will be described in detail later.

Our goal is to study the efficiency of A-AMEM when compared to A-EM for different initial number of Gaussians components, K_{init} . To this end, we define the iteration reduction factor (IRF) and CPU time reduction factor (TRF) between accelerated and non-accelerated EM algorithms as:

$$IRF = \frac{\text{number of standard EM iterations}}{\text{number of accelerated EM iterations}}, \quad (24)$$

$$TRF = \frac{\text{standard EM CPU time}}{\text{accelerated EM CPU time}}. \quad (25)$$

The same terminating tolerance is used when applying both A-AMEM and A-EM to the data sets. In order for both A-EM and A-AMEM to kill enough unnecessary components before converging to the desired optimal solutions, we use a small terminating tolerance TOL . In particular, we set $TOL = 10^{-10}$ for the synthetic data sets, and $TOL = 10^{-12}$ for the PIC data sets.

As for the choice of m_{AA} , the maximum number of past residuals in AA, we acknowledge that the performance of AA with respect to this number is problem-dependent, which was also remarked in [54]. We find that using m_{AA} between 5 and 10 works well for our simulations. We set $m_{AA} = 5$ for $K_{init} = 3$, and $m_{AA} = 10$ for $3 < K_{init} \leq 10$.

5.1 Visualization of the manufactured GMM data sets

The 2D view of the synthetic data sets in the X-Y plane is given in Fig. 1. The views in the Y-Z and X-Z planes are identical to the X-Y plane's view, since we use diagonal covariance matrices for the three components in the mixture.

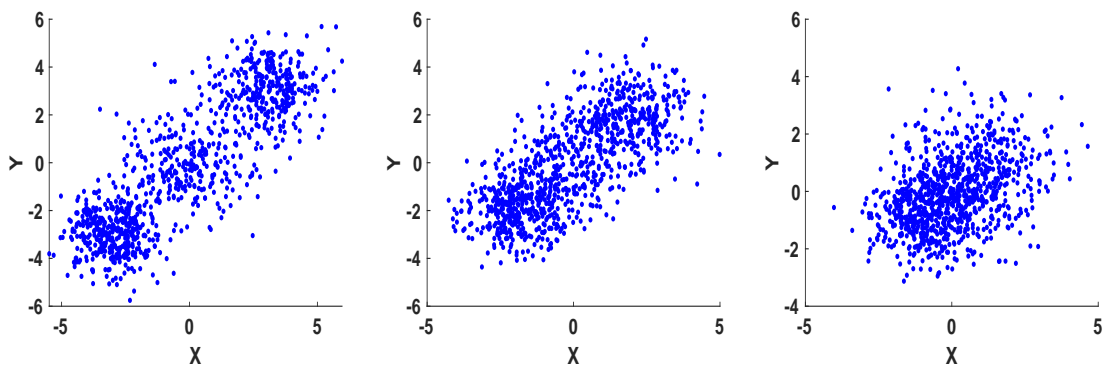


Fig. 1. Visualization of manufactured GMM data sets in the X-Y plane. (Left) VWS data set. (Center) PS data set. (Right) VPS data set.

We can clearly observe the presence of the three Gaussian components in the VWS data set and somewhat clearly in the PS data set. However, they are impossible to tell by the naked eye in the VPS data set. It is expected that A-EM will be able to detect the right number of components and converge fairly quickly for the VWS data set. It is also anticipated that A-EM will detect the right number of Gaussians for the PS data set but with a slower convergence rate. For the VPS data set, however, A-EM is expected to converge extremely slowly due to the significant overlap among Gaussian components in the mixture, and perhaps even underestimate the number of components.

5.2 Performance of the non-adaptive ELS-EM

We illustrate the performance of ELS-EM for GMM by applying it to the synthetic data sets in Section 5.1 and comparing the results with standard EM. For these tests, we use $K_{init} = 3$, fixed, i.e., we assume the exact model. We use the same tolerance for terminating both algorithms. Both ELS-EM and standard EM are initialized using the best K-means result, i.e., with the smallest inertia (SSE) values, out of multiple trials with $K = 3$ clusters, as described in Section 4.2. In these simulations, we note that ELS-EM converges to the same solutions as EM. We report the ratios for IRF and TRF between ELS-EM and EM in Table 1. We observe from the Table that the ratios of IRF over TRF are approximately equal to 2.0. This verifies that, on average, one iteration of ELS-EM is twice as expensive as one iteration of EM. It is also apparent that ELS-ES is only able to speed up the convergence by a factor of $\lesssim 2$ for all cases, resulting in no actual CPU speed up (as demonstrated by the TRF values in Table 1).

TABLE 1
Reduction factors for ELS-EM.

	IRF	TRF	IRF/TRF
VWS	1.50	0.81	1.85
PS	1.90	0.89	2.13
VPS	1.89	0.90	2.10

5.3 Application of A-AMEM to manufactured data sets with $K_{init} = 3$

We apply A-EM and A-AMEM to the manufactured data sets using the exact initial number of components $K_{init} = 3$. We initialize the Gaussians as in the previous section. Fig. 2 depicts the convergence history of the log-likelihood of the two algorithms. We have added a subplot inside the convergence plot of the VPS case to zoom into the first 40 iterations.

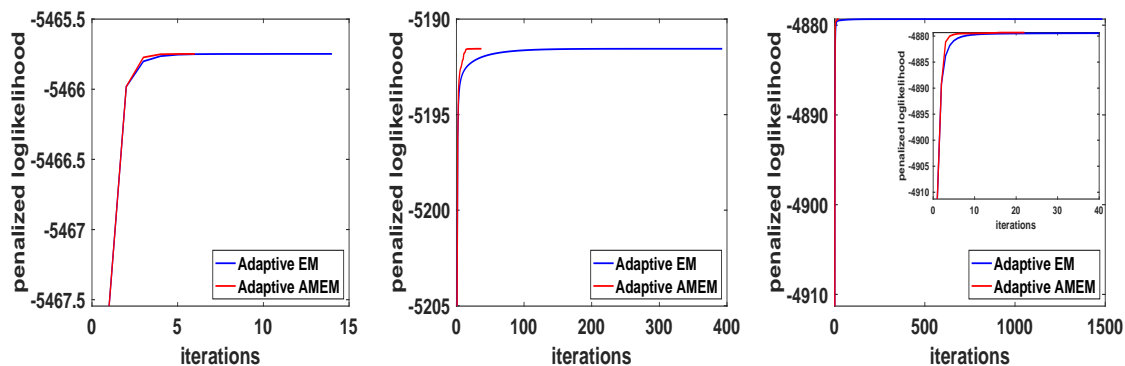


Fig. 2. Case $K_{init} = 3$: History of penalized log-likelihood values as a function of the number of iterations for synthetic data sets. (Left) VWS data set. (Center) PS data set. (Right) VPS data set.

As expected, the convergence rate of A-EM worsens with increasing Gaussian-component overlap. However, A-AMEM seems to converge fairly quickly, regardless of component overlap, to the same penalized log-likelihood values as the non-accelerated version. We also remark that both A-EM and A-AMEM give the correct number of components ($K_{final} = 3$) for the three manufactured data sets, i.e., both algorithms are able to recognize the true number of components within each data set and do not kill any component. Table 2 records the iteration and the wall-clock time reduction factors for this case, and shows that A-AMEM outperforms A-EM dramatically, especially for the hard VPS case (by a factor of 60 in wall-clock time).

5.4 A failed application of AA without monotonicity control to A-EM

In practice, we often do not know in advance the exact model of the Gaussian mixtures. Therefore, it is wise to start with a number of Gaussian components larger than the suspected number of groups, and rely on component adaptivity to find the correct model. However, the application of AA without monotonicity control to A-EM (which we term A-AAEM) fails catastrophically. To demonstrate this, we compare the outcomes of A-EM with and without AA (with no

TABLE 2
Reduction factors for $K_{init} = 3$.

	IRF	TRF	IRF/TRF
VWS	2.33	1.98	1.18
PS	10.62	10.22	1.04
VPS	67.45	60.96	1.11

monotonicity control) to the synthetic data sets with $K_{init} = 5$. Gaussian parameters are initialized from the best run out of multiple trials of K-means clustering with $K = 5$ clusters. The histories of the penalized log-likelihood values as a function of the number of iterations are given in Fig. 3.

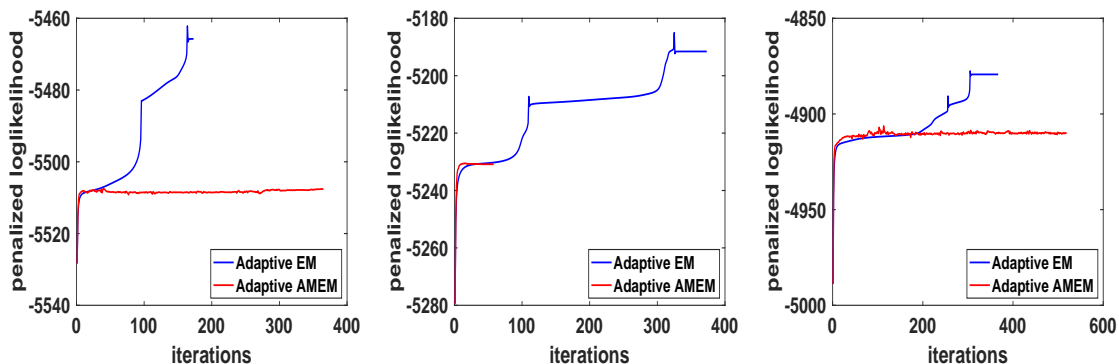


Fig. 3. Case $K_{init} = 5$ – Application of AA to A-EM without monotonicity control: History of penalized log-likelihood values as a function of the number of iterations for synthetic data sets. (Left) VWS data set. (Center) PS data set. (Right) VPS data set.

From the figure, we observe that A-AAEM fails to annihilate unnecessary Gaussian components, converges to the wrong solutions, and sometimes is even slower than the non-accelerated version. Using $K_{init} > K_{exact}$ is equivalent to expanding the solution space, i.e., many local maxima are created, and the accelerated A-EM manages to converge to one of those local maxima in the expanded subspace. That AA+EM finds a suboptimal solution is also the case without EM adaptivity (AAEM) when $K_{init} > K_{exact}$, even if standard EM is able to find the correct solution. More specifically, in our simulations with $K_{init} = 5 > K_{exact}$, standard EM finds three Gaussians approximately matching the exact ones, and two Gaussians with very small weights. However, in the converged AAEM solutions, we observe that all five Gaussians have comparable weights, and the means and covariance matrices for these Gaussians are far from the exact parameters. As a result, at convergence, $\mathcal{L}(\theta(\text{AAEM})) < \mathcal{L}(\theta(\text{EM}))$ for the standard case and $\mathcal{P}\mathcal{L}(\theta(\text{A-AAEM})) < \mathcal{P}\mathcal{L}(\theta(\text{A-EM}))$ for the adaptive case, as we observed in Fig. 3. We conclude that the application of AA to EM-GMM without monotonicity control yields unreliable solutions and no performance advantage when the exact number of components in the mixture is unknown.

5.5 Application of AA to A-EM with monotonicity control (A-AMEM) to manufactured data sets with $K_{init} = 5$

We use $K_{init} = 5$ in both A-AMEM and A-EM, and the initialization of Gaussian parameters is done in the same manner as described in Section 5.4. Note that we turn on the monotonicity control step for this test. As shown in Fig. 4, both algorithms can detect the right number of Gaussian components at convergence for the manufactured data sets, and find the same solution. A-AMEM is able to annihilate Gaussian components somewhat faster than A-EM, but converges very fast once the optimal number of Gaussian components is reached, while A-EM continues to struggle to converge, especially for the VPS data set.

We also investigate the dynamics of the component removal process in A-AMEM due to the monotonicity control step. To this end, in Fig. 5 we show the binary plots of the solution choices, AA iterate or EM iterate, during the A-AMEM iteration for the three synthetic GMM data sets. In the binary plots, the y-value for a given iteration is set to 0 only when A-AMEM falls back to the EM solution due to lack of monotonicity (and not because of violations of positivity). Also, the vertical lines in these binary plots represent the iterations when Gaussians are killed.

From Fig. 5 we see that A-AMEM frequently reverts back to EM before reaching the optimal number of Gaussian components in order to maintain the monotonicity of the penalized log-likelihood function. This explains the fact that A-AMEM kills Gaussian components at a comparable rate to A-EM. However, once the optimal number of components is reached, the acceleration kicks in aggressively and A-AMEM barely rolls back to EM. The last dot (with y-value equal to zero) in each of the binary plots of Fig. 5 indicates the application of a final standard EM step for conservation up to the second moments of the data points [17].

Table 3 shows the IRF and TRF for $K_{init} = 5$, demonstrating that A-AMEM converges faster than A-EM, especially for the hard VPS data set, with speed-ups reaching an order of magnitude for that case.

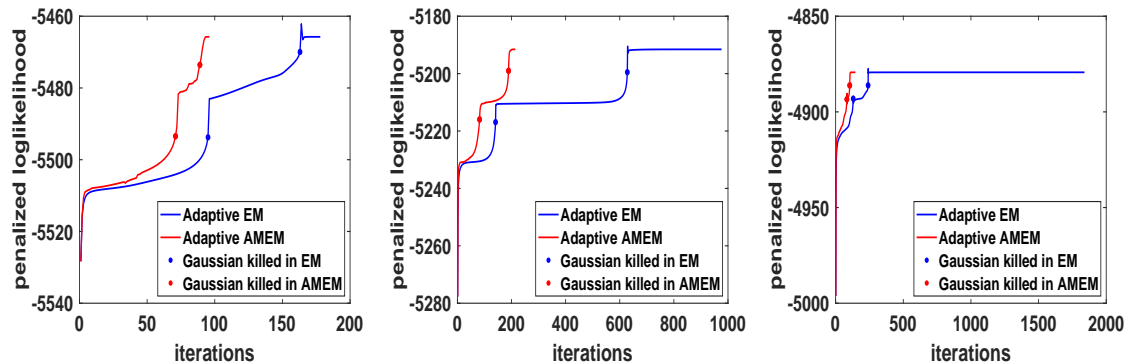


Fig. 4. Case $K_{init} = 5$: History of penalized log-likelihood values as a function of the number of iterations for synthetic data sets. (Left) VWS data set. (Center) PS data set. (Right) VPS data set. The blue and red dots indicate the iterations where Gaussians are killed.

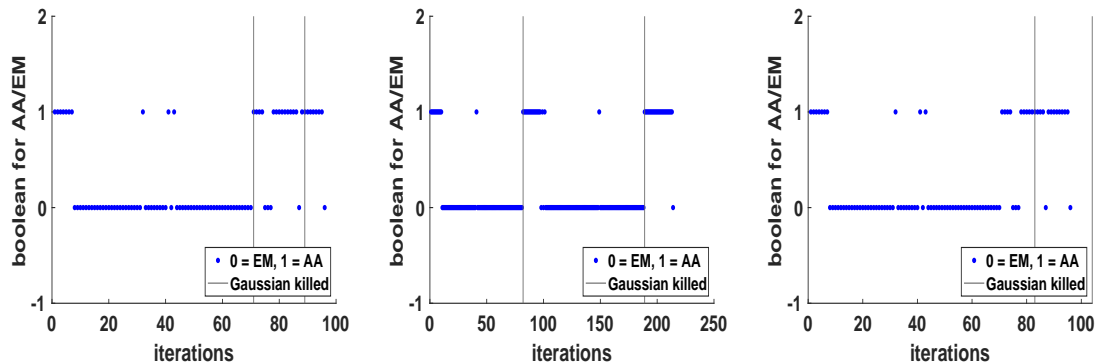


Fig. 5. Case $K_{init} = 5$: History of solution choices in A-AMEM iterations for synthetic data sets. (Left) VWS data set. (Center) PS data set. (Right) VPS data set.

TABLE 3
Reduction factors for $K_{init} = 5$.

	IRF	TRF	IRF/TRF
VWS	1.85	1.83	1.01
PS	4.56	3.94	1.16
VPS	12.60	10.01	1.26

5.6 Application of A-AMEM with monotonicity control to manufactured data sets with $K_{init} = 8$

Next, we consider $K_{init} = 8$, and perform the same numerical simulations for the manufactured GMM data set using both adaptive non-accelerated and accelerated EM. As before, Gaussian parameters are initialized from the best run out of multiple runs of K-means clustering, but with $K = 8$ clusters. We present the plots of the penalized log-likelihood values as a function of the number of iterations in Fig. 6.

Observations for this case are very similar to the $K_{init} = 5$ case. Again, in the beginning A-AMEM kills Gaussian components at a similar rate to A-EM. However, once the optimal number of Gaussian components is reached, A-AMEM quickly converges while A-EM struggles. In terms of accuracy, both A-AMEM and A-EM converge to the same solutions and yield the same final penalized log-likelihood value. The IRF and TRF for this case are presented in Table 4, again demonstrating a significant speed-up.

It is clear from Figs. 4 and 6 that A-AMEM does not remove Gaussian components much more efficiently than A-EM. Since a larger K_{init} requires more Gaussian killing, it delays the onset of the fast convergence stage of the iteration, resulting in the increase (degradation) of the IRF/TRF ratio between the $K_{init} = 5$ and $K_{init} = 8$ cases observed in Tables 3 and 4. This result highlights the importance of finding good guesses for the initial number of components. We will discuss in detail our strategy for finding best guess for K_{init} in Section 5.9.

5.7 Performance of A-AMEM without Taylor expansion in the monotonicity control step

Previous results in Section 5.5 and Section 5.6 have demonstrated that the cost per iteration of A-AMEM is comparable to A-EM. To further highlight the importance of using the Taylor expansion for the monotonicity control step, we examine the performance of A-AMEM (vs. A-EM) using (19) instead of (20). This requires an extra evaluation of the penalized log-likelihood function (9) at every A-AMEM iteration. We consider the synthetic data sets with $K_{init} = 5$

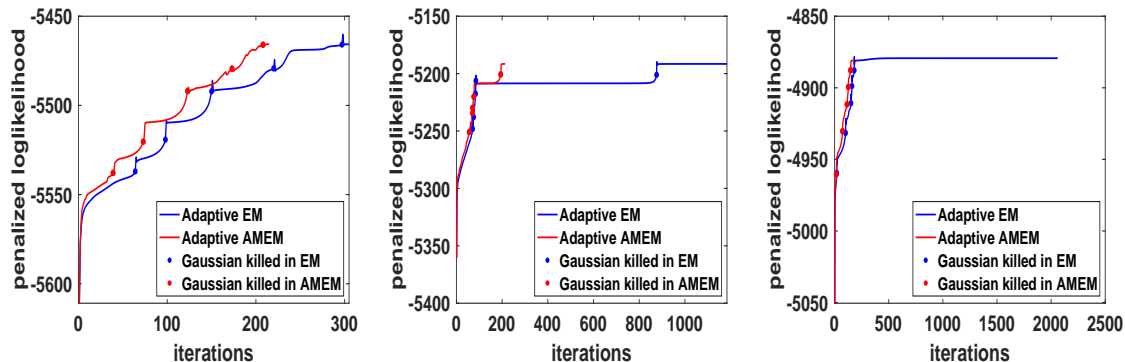


Fig. 6. Case $K_{init} = 8$: History of penalized log-likelihood values as a function of the number of iterations for synthetic data sets. (Left) VWS data set. (Center) PS data set. (Right) VPS data set. The blue and red dots indicate the iterations where Gaussians are killed.

TABLE 4
Reduction factors for $K_{init} = 8$.

	IRF	TRF	IRF/TRF
VWS	1.42	1.46	0.97
PS	5.56	4.12	1.35
VPS	11.26	6.73	1.67

and $K_{init} = 8$. Table 5 shows that the IRF/TRF ratios for these cases are ~ 2 , confirming that one iteration of A-AMEM without Taylor expansion is about twice as expensive as one A-EM iteration.

TABLE 5
Reduction factors for $K_{init} = 5, 8$ without using Taylor expansion in the monotonicity control step.

	$K_{init} = 5$			$K_{init} = 8$		
	IRF	TRF	IRF/TRF	IRF	TRF	IRF/TRF
VWS	1.73	1.01	1.71	1.44	0.88	1.64
PS	4.51	2.43	1.86	4.45	2.11	2.11
VPS	10.90	5.07	2.15	8.63	3.78	2.28

5.8 Application of A-AMEM to particle-in-cell (PIC) data sets

As a final test for A-AMEM, we consider data sets generated from PIC simulations (see [74] for detailed description of PIC and [17] for a specific PIC application of GMM). In particular, we consider the same 2D-3V Weibel electromagnetic instability [75] as in Ref. [17]. We partition the 2D spatial domain into 16×16 cells, with $N \approx 1024$ particles per cell per species. We run the simulations until time $t = 50$ (in inverse plasma frequency units) and record the velocity points of all particles within each cell. The particle velocities in the 3D velocity space in each cell provide the data set. We then test the algorithms with selected cells. By applying both A-AMEM and A-EM to these cells, we assume that the velocity distribution functions (VDFs) can be approximated by a Gaussian mixture model of unknown number of components. At time $t = 50$, the simulations are in the nonlinear phase and the electron VDFs strongly deviate from the Maxwellian distribution. Therefore, for most of the cells, we expect at least a few (anisotropic) components.

For demonstration purposes, we choose cells 83, 155, 170, 243, with the cell numbers defined lexicographically on the 2D spatial mesh from-left-to-right and from-bottom-to-top. We apply A-EM and A-AMEM to these data sets using $K_{init} = 8$ and $K_{init} = 10$ Gaussian components. The plots of penalized log-likelihood values as functions of iterations are given in Fig. 7 and the IRFs and TRFs are recorded in Table 6.

TABLE 6
Reduction factors for $K_{init} = 8, 10$ for particle-in-cell data sets.

	$K_{init} = 8$			$K_{init} = 10$		
	IRF	TRF	IRF/TRF	IRF	TRF	IRF/TRF
Cell 83	2.25	1.95	1.15	2.97	2.54	1.17
Cell 155	7.15	6.16	1.16	5.09	4.21	1.21
Cell 170	3.69	3.25	1.14	4.52	3.10	1.46
Cell 243	3.86	3.34	1.16	4.46	3.03	1.47

We observe from Fig. 7 and Table 6 that A-AMEM converges two to six times faster than A-EM to the same solution, and that on average the largest accelerations and smaller IRF/TRF ratios occur for smaller K_{init} , again emphasizing the need for good initial guesses for the number of components to maximize performance.

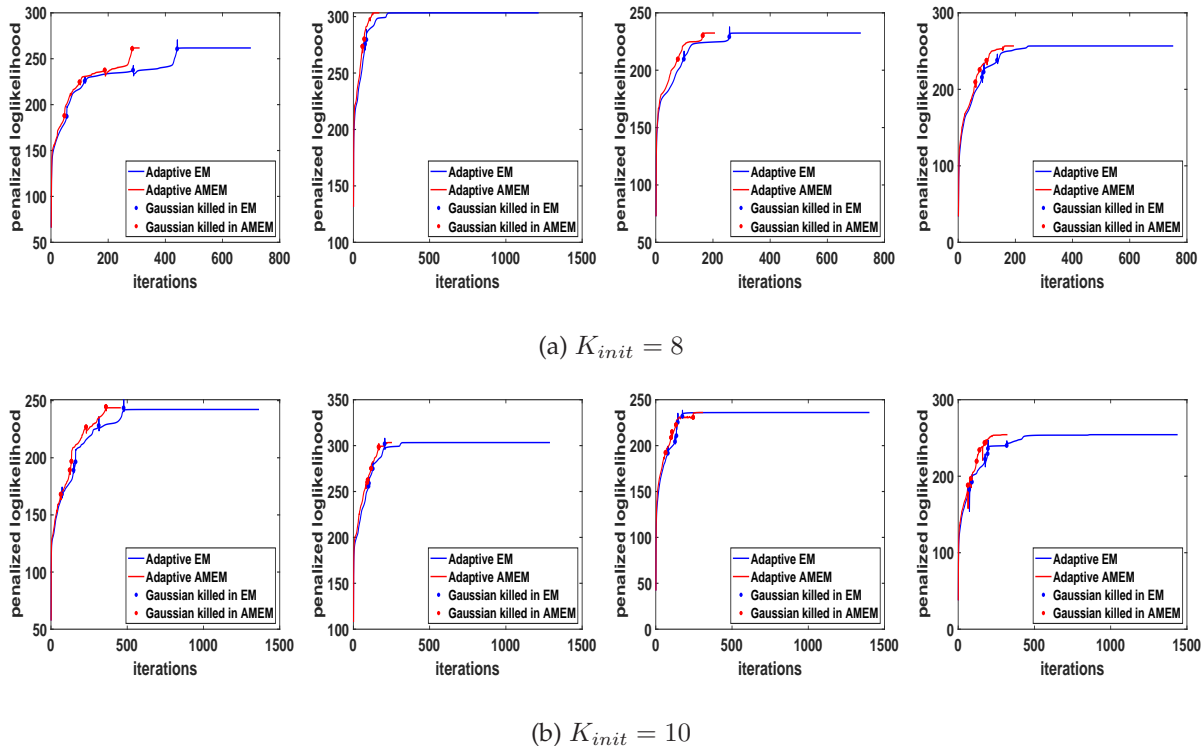


Fig. 7. Application of A-AMEM for PIC data sets with $K_{init} = 8, 10$: History of penalized log-likelihood values as a function of the number of iterations for selected particle-in-cell data sets. (From left to right) Cell 83, 155, 170, 243. The blue and red dots indicate the iterations where Gaussians are killed.

5.9 Gap-statistic K-Means multi-initialization strategy

The previous results highlight the importance of choosing K_{init} wisely. In addition to the gap statistic (GS) method, we have explored other extensions of K-means clustering algorithms proposed in the literature [62], [63], [65], [66] to obtain a good initial guess of the number of components for both A-EM and A-AMEM. Firstly, we tested the so-called map-dp clustering method introduced in [62]. This approach works well for well separated data sets but not for poorly separated ones. We observed that, when the Gaussians are poorly separated, this approach usually yields a single $K = 1$ component. In addition, the effectiveness of the approach strongly depends on the choice of parameters, making it brittle. Secondly, we tried the mean silhouette approach [64]–[66]. This approach works well for our data sets. However, it is very expensive since it requires distance evaluation between all points in the data sets, i.e., it has computational complexity of order $O(N^2D)$, much greater than the complexity of the K-means algorithm, $O(NKD)$ for $N \gg K$.

We find that GS [56] is cheap to use with K-means as the clustering method, and gives good estimates for the initial number of components for our data sets (as we show below). The initialization procedure for the Gaussian parameters using GS (as described in Section 4.2) is summarized in Algorithm 3. We use $K_{min} = 2$, $K_{max} = 10$, and $K_{adjust} = 2$ for our numerical simulations.

Algorithm 3 GS-K-means algorithm

Given data set $\mathbf{X} = (\mathbf{x}_1, \dots, \mathbf{x}_N)$, the minimum number of cluster K_{min} and the maximum number of cluster K_{max}

- 1) Use the gap statistic (GS) method [56] to estimate the number of components among K_{min}, \dots, K_{max} clusters, i.e., $K_{opt} = \text{GS-method}(K_{min}, K_{max})$.
 - 2) Set $K_{init} = K_{opt} + K_{adjust}$ for some $K_{adjust} > 0$ to further avoid possible under-estimations.
 - 3) Perform K-means algorithm using K_{init} clusters multiple times and select centroids from the best run which yields the smallest inertia (SSE).
 - 4) Set the initial means to be the centroids obtained from Step 3 and compute the initial values for Gaussian weights and covariance matrices.
-

Fig. 8 shows the results for the number of components from the GS-K-means method for the synthetic data sets. Table 7 presents numerical results for applying A-EM and A-AMEM initialized with GS-K-means to both synthetic and PIC data sets. We remark that in these simulations, A-EM and A-AMEM converge to the same solutions. We observe that the number of components returned by the GS-K-means initialization for the synthetic data set is very accurate

for the VWS and PS data sets. For the VPS data set, since the Gaussians are highly overlapping, the method underestimates the number of components by only one. For the synthetic tests, the optimal final number of components K_{final} returned by A-EM and A-AMEM is equal to the number of components predicted by GS-K-means. For the PIC data sets, we observe that the GS-K-means underestimates the optimal number of components by one or two groups, justifying the need to adjust K_{est} by some amount K_{adjust} in Alg. 3.

Finally, we note that on average the wall-clock-time for the GS-K-means initialization step is about an order of magnitude smaller than adaptive EM in our experiments, but this cost is likely amortized by the performance gains from accurately guessing the number of components of the mixture.

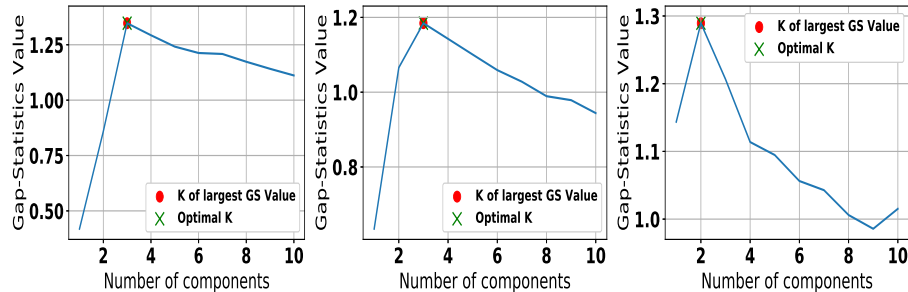


Fig. 8. Estimated number of components by GS-K-means for synthetic data sets. (Left) VWS data set. (Center) PS data set. (Right) VPS data set.

TABLE 7

Results of using A-EM and A-AMEM with GS-K-means for both synthetic and particle-in-cell data sets. K_{final} is the optimal number of groups returned by both A-EM and A-AMEM.

	K_{est}	K_{init}	IRF	TRF	K_{final}
VWS	3	5	1.85	1.76	3
PS	3	5	4.39	4.03	3
VPS	2	4	2.28	2.08	2
Cell 83	2	4	1.84	1.87	3
Cell 155	2	4	12.02	11.85	4
Cell 170	3	5	4.80	4.53	5
Cell 243	2	4	3.63	3.26	3

6 CONCLUSION

We propose for the first time an accelerated, monotonicity-preserving algorithm for the *adaptive* EM-GMM algorithm that is significantly faster (in wall-clock time) than its non-accelerated counterpart. The method combines the minimum-message-length Bayesian information criterion with a monotonicity-controlled Anderson acceleration (AA) solver. The targeted use of exact score functions in the monotonicity control step of AA avoids computations of the log-likelihood function, which is very expensive for GMM, and delivers an overall very competitive method. The resulting A-AMEM converges to the same solution as the non-accelerated version, strictly conserves up to second moments of the observed data points and ensures the positive-definiteness property of the solutions. The method has been tested on several synthetic and data sets generated from PIC simulations. It shows significant acceleration (from a few times up to more than an order of magnitude) in terms of both iteration count and wall-clock time. Finally, we have explored the use of a GS-K-means initialization strategy, which provides as good a guess for the number of components as practical at a fraction of the cost of the adaptive EM algorithm. By eliminating the guess work in the number of components (and thus avoiding the necessary culling of unneeded mixture components), this strategy significantly enhances both the efficiency and robustness of our approach in practical applications.

APPENDIX

DERIVATION OF THE DERIVATIVES OF LOG-LIKELIHOOD FUNCTION W.R.T GAUSSIAN PARAMETERS

We consider the log-likelihood function with particle weight ζ_j for all $j = 1, \dots, N$ as follows:

$$\mathcal{L}(\theta) = \sum_{j=1}^N \zeta_j \ln \left(\sum_{k=1}^K \omega_k G_k(\mathbf{x}_j; \boldsymbol{\mu}_k, \boldsymbol{\Sigma}_k) \right) + \eta \left(\sum_{k=1}^K \omega_k - 1 \right) \quad (26)$$

where N is the total number of observed points in the data set, K is the number of Gaussian components in the mixture and $\mathbf{x}_j, j = 1, \dots, N$ is the observed data points with weights ζ_j , and $\eta \left(\sum_{k=1}^K \omega_k - 1 \right)$ is the Lagrange multiplier

term that enforces the normalization constraint $\sum_{k=1}^K \omega_k = 1$. We assume that $\sum_{j=1}^N \zeta_j = N$. Parameters ω_k , $\boldsymbol{\mu}_k$ and $\boldsymbol{\Sigma}_k$ represent the weights, means, and covariance matrices of the k th Gaussian. The Gaussian distribution k th in the D -dimensional space is defined as

$$G_k(\mathbf{x}; \boldsymbol{\mu}_k, \boldsymbol{\Sigma}_k) = \frac{1}{\sqrt{(2\pi)^D |\boldsymbol{\Sigma}_k|}} e^{-\frac{1}{2}(\mathbf{x} - \boldsymbol{\mu}_k)^T \boldsymbol{\Sigma}_k^{-1} (\mathbf{x} - \boldsymbol{\mu}_k)}. \quad (27)$$

Firstly, we employ the following identities from the Matrix Cook Book [76]:

$$\frac{\partial}{\partial \mathbf{s}} (\mathbf{x} - \mathbf{s})^T \mathbf{W} (\mathbf{x} - \mathbf{s}) = -2\mathbf{W} (\mathbf{x} - \mathbf{s}), \quad (28)$$

$$\frac{\partial}{\partial \mathbf{A}} \mathbf{v}^T \mathbf{A}^{-1} \mathbf{v} = -\mathbf{A}^{-1} \mathbf{v} \mathbf{v}^T \mathbf{A}^{-1}, \quad (29)$$

$$\frac{\partial}{\partial \mathbf{A}} |\mathbf{A}| = |\mathbf{A}| \mathbf{A}^{-1}. \quad (30)$$

where \mathbf{x} , \mathbf{s} are vectors and \mathbf{W} , \mathbf{A} are matrices.

Secondly, we define the following quantities

$$f(\mathbf{x}_j) = f(\mathbf{x}_j; \boldsymbol{\theta}) = \sum_{l=1}^K \omega_l G_l(\mathbf{x}_j; \boldsymbol{\mu}_l, \boldsymbol{\Sigma}_l), \quad (31)$$

$$r_{jk} = \frac{\zeta_j \omega_k G_k(\mathbf{x}_j; \boldsymbol{\mu}_k, \boldsymbol{\Sigma}_k)}{f(\mathbf{x}_j)}, \quad (32)$$

where $\boldsymbol{\theta} = (\boldsymbol{\theta}_1, \dots, \boldsymbol{\theta}_K)$, $k = 1, \dots, K$ and $\boldsymbol{\theta}_k = (\omega_k, \boldsymbol{\mu}_k, \boldsymbol{\Sigma}_k)$. K is the total number of components in the Gaussian mixture (GM).

Next, taking the derivative of $\mathcal{L}(\boldsymbol{\theta})$ w.r.t. the mean $\boldsymbol{\mu}_k$, we have

$$\begin{aligned} \frac{\partial \mathcal{L}(\boldsymbol{\theta})}{\partial \boldsymbol{\mu}_k} &= \sum_{j=1}^N \frac{\zeta_j}{f(\mathbf{x}_j)} \frac{\partial}{\partial \boldsymbol{\mu}_k} \left[\frac{\omega_k e^{-\frac{1}{2}(\mathbf{x}_j - \boldsymbol{\mu}_k)^T \boldsymbol{\Sigma}_k^{-1} (\mathbf{x}_j - \boldsymbol{\mu}_k)}}{(2\pi)^{D/2} |\boldsymbol{\Sigma}_k|^{1/2}} \right] \\ &= \sum_{j=1}^N \frac{\zeta_j \omega_k G_k(\mathbf{x}_j; \boldsymbol{\mu}_k, \boldsymbol{\Sigma}_k)}{f(\mathbf{x}_j)} \times \\ &\quad \frac{\partial \left(-\frac{1}{2}(\mathbf{x}_j - \boldsymbol{\mu}_k)^T \boldsymbol{\Sigma}_k^{-1} (\mathbf{x}_j - \boldsymbol{\mu}_k) \right)}{\partial \boldsymbol{\mu}_k} \\ &= \sum_{j=1}^N -\frac{r_{jk}}{2} \frac{\partial}{\partial \boldsymbol{\mu}_k} \left((\mathbf{x}_j - \boldsymbol{\mu}_k)^T \boldsymbol{\Sigma}_k^{-1} (\mathbf{x}_j - \boldsymbol{\mu}_k) \right) \\ &= \sum_{j=1}^N r_{jk} \boldsymbol{\Sigma}_k^{-1} (\mathbf{x}_j - \boldsymbol{\mu}_k). \end{aligned} \quad (33)$$

where in the last equality of (33), we use (28).

Taking the derivative of $\mathcal{L}(\boldsymbol{\theta})$ w.r.t. the covariance matrix $\boldsymbol{\Sigma}_k$, we have

$$\begin{aligned} \frac{\partial \mathcal{L}(\boldsymbol{\theta})}{\partial \boldsymbol{\Sigma}_k} &= \sum_{j=1}^N \frac{\zeta_j}{f(\mathbf{x}_j)} \frac{\partial}{\partial \boldsymbol{\Sigma}_k} \left[\frac{\omega_k e^{-\frac{1}{2}(\mathbf{x}_j - \boldsymbol{\mu}_k)^T \boldsymbol{\Sigma}_k^{-1} (\mathbf{x}_j - \boldsymbol{\mu}_k)}}{(2\pi)^{D/2} |\boldsymbol{\Sigma}_k|^{1/2}} \right] \\ &= \sum_{j=1}^N \frac{\zeta_j \omega_k}{f(\mathbf{x}_j)} \left\{ \frac{e^{-\frac{1}{2}(\mathbf{x}_j - \boldsymbol{\mu}_k)^T \boldsymbol{\Sigma}_k^{-1} (\mathbf{x}_j - \boldsymbol{\mu}_k)}}{(2\pi)^{D/2}} \frac{\partial |\boldsymbol{\Sigma}_k|^{-\frac{1}{2}}}{\partial \boldsymbol{\Sigma}_k} \right. \\ &\quad \left. + G_k(\mathbf{x}_j; \boldsymbol{\mu}_k, \boldsymbol{\Sigma}_k) \frac{\partial}{\partial \boldsymbol{\Sigma}_k} \left[-\frac{1}{2}(\mathbf{x}_j - \boldsymbol{\mu}_k)^T \boldsymbol{\Sigma}_k^{-1} (\mathbf{x}_j - \boldsymbol{\mu}_k) \right] \right\} \\ &= \sum_{j=1}^N \frac{\zeta_j \omega_k}{f(\mathbf{x}_j)} \left\{ -\frac{1}{2} G_k(\mathbf{x}_j; \boldsymbol{\mu}_k, \boldsymbol{\Sigma}_k) \boldsymbol{\Sigma}_k^{-1} \right. \\ &\quad \left. + \frac{1}{2} G_k(\mathbf{x}_j; \boldsymbol{\mu}_k, \boldsymbol{\Sigma}_k) \boldsymbol{\Sigma}_k^{-1} (\mathbf{x}_j - \boldsymbol{\mu}_k) (\mathbf{x}_j - \boldsymbol{\mu}_k)^T \boldsymbol{\Sigma}_k^{-1} \right\} \\ &= \sum_{j=1}^N \frac{r_{jk}}{2} \left\{ -\boldsymbol{\Sigma}_k^{-1} + \boldsymbol{\Sigma}_k^{-1} (\mathbf{x}_j - \boldsymbol{\mu}_k) (\mathbf{x}_j - \boldsymbol{\mu}_k)^T \boldsymbol{\Sigma}_k^{-1} \right\}, \end{aligned} \quad (34)$$

in which we use (29) and (30) to go from the second equality to the third equality.

Taking the derivative of $\mathcal{L}(\boldsymbol{\theta})$ w.r.t. the weight ω_k subject to the constraint $\sum_{k=1}^K \omega_k = 1$, we have

$$\begin{aligned} \frac{\partial \mathcal{L}(\boldsymbol{\theta})}{\partial \omega_k} &= \frac{\partial}{\partial \omega_k} \left\{ \sum_{j=1}^N \zeta_j \ln \left(\sum_{k=1}^K \omega_k G_k(\mathbf{x}_j; \boldsymbol{\mu}_k, \boldsymbol{\Sigma}_k) \right) \right. \\ &\quad \left. + \eta \left(\sum_{k=1}^K \omega_k - 1 \right) \right\} \\ &= \sum_{j=1}^N \frac{\zeta_j G_k(\mathbf{x}_j; \boldsymbol{\mu}_k, \boldsymbol{\Sigma}_k)}{f(\mathbf{x}_j)} + \eta \\ &= \frac{1}{\omega_k} \sum_{j=1}^N r_{jk} + \eta, \end{aligned} \quad (35)$$

where $\eta = -N$ in (35). In the case of the penalized log-likelihood function, taking into account the penalized terms, we have

$$\begin{aligned} \frac{\partial \mathcal{L}(\boldsymbol{\theta})}{\partial \omega_k} &= \frac{\partial}{\partial \omega_k} \left\{ \sum_{j=1}^N \zeta_j \ln \left(\sum_{k=1}^K \omega_k G_k(\mathbf{x}_j; \boldsymbol{\mu}_k, \boldsymbol{\Sigma}_k) \right) \right. \\ &\quad \left. - \frac{T}{2} \sum_{k=1}^K \ln(\omega_k) + \eta \left(\sum_{k=1}^K \omega_k - 1 \right) \right\} \\ &= \sum_{j=1}^N \frac{\zeta_j G_k(\mathbf{x}_j; \boldsymbol{\mu}_k, \boldsymbol{\Sigma}_k)}{f(\mathbf{x}_j)} - \frac{T}{2\omega_k} + \eta \\ &= \frac{1}{\omega_k} \sum_{j=1}^N r_{jk} - \frac{T}{2\omega_k} + \eta, \end{aligned} \quad (36)$$

where $\eta = -N + 0.5TK$ for this case.

Setting (33), (34), and (35) equal to zero and using $\eta = -N$, we arrive at

$$\boldsymbol{\Sigma}_k^{-1} \left(\sum_{j=1}^N r_{jk} (\mathbf{x}_j - \boldsymbol{\mu}_k) \right) = 0 \Leftrightarrow \boldsymbol{\mu}_k = \frac{\sum_{j=1}^N r_{jk} \mathbf{x}_j}{\sum_{j=1}^N r_{jk}}, \quad (37)$$

$$\begin{aligned} \boldsymbol{\Sigma}_k^{-1} \left(\sum_{j=1}^N \frac{r_{jk}}{2} \left\{ -\boldsymbol{\Sigma}_k + (\mathbf{x}_j - \boldsymbol{\mu}_k)(\mathbf{x}_j - \boldsymbol{\mu}_k)^T \right\} \right) \boldsymbol{\Sigma}_k^{-1} &= 0 \\ \Leftrightarrow \boldsymbol{\Sigma}_k &= \frac{\sum_{j=1}^N r_{jk} (\mathbf{x}_j - \boldsymbol{\mu}_k)(\mathbf{x}_j - \boldsymbol{\mu}_k)^T}{\sum_{j=1}^N r_{jk}}, \end{aligned} \quad (38)$$

and

$$\frac{1}{\omega_k} \sum_{j=1}^N r_{jk} = -\eta = N \Leftrightarrow \omega_k = \frac{\sum_{j=1}^N r_{jk}}{N}. \quad (39)$$

Similarly, for the penalized log-likelihood case, setting (36) to zero and using $\eta = -N + 0.5TK$, we have

$$\begin{aligned} \frac{1}{\omega_k} \sum_{j=1}^N r_{jk} - \frac{T}{2\omega_k} &= -\eta = N - 0.5TK \\ \Leftrightarrow \omega_k &= \frac{\sum_{j=1}^N r_{jk} - 0.5T}{N - 0.5TK}. \end{aligned} \quad (40)$$

Here, we note that $\frac{\partial \mathcal{L}(\boldsymbol{\theta})}{\partial \boldsymbol{\mu}_k} = \frac{\partial \mathcal{P}\mathcal{L}(\boldsymbol{\theta})}{\partial \boldsymbol{\mu}_k}$ and $\frac{\partial \mathcal{L}(\boldsymbol{\theta})}{\partial \boldsymbol{\Sigma}_k} = \frac{\partial \mathcal{P}\mathcal{L}(\boldsymbol{\theta})}{\partial \boldsymbol{\Sigma}_k}$.

ACKNOWLEDGMENT

This work was supported by the U.S. Department of Energy, Office of Science, through the Scientific Discovery through Advanced Computation (SciDAC) Fusion Energy Sciences/Applied Scientific Computing Research partnership program. This research used resources provided by the Los Alamos National Laboratory Institutional Computing Program, and was performed under the auspices of the National Nuclear Security Administration of the U.S. Department of Energy at Los Alamos National Laboratory, managed by Triad National Security, LLC under contract 89233218CNA000001.

REFERENCES

- [1] D. M. Titterton, A. F. Smith, and U. E. Makov, *Statistical analysis of finite mixture distributions*. Wiley, 1985.
- [2] G. J. McLachlan and D. Peel, *Finite mixture models*, ser. Wiley series in probability and statistics: Applied probability and statistics. John Wiley & Sons, 2004.
- [3] G. J. McLachlan, S. X. Lee, and S. I. Rathnayake, "Finite mixture models," *Annual review of statistics and its application*, vol. 6, pp. 355–378, 2019.
- [4] S. Fruhwirth-Schnatter, G. Celeux, and C. P. Robert, *Handbook of mixture analysis*. CRC press, 2019.
- [5] C. M. Bishop, *Pattern recognition and machine learning (Information science and statistics)*. Berlin, Heidelberg: Springer-Verlag, 2006.
- [6] K. P. Murphy, *Machine learning: A probabilistic perspective*. MIT Press, 2012.
- [7] S. Liu, J. McGree, Z. Ge, and Y. Xie, *Computational and statistical methods for analysing big data with applications*. Academic Press, 2016.
- [8] I. Ullah and K. Mengersen, "Bayesian mixture models and their big data implementations with application to invasive species presence-only data," *Journal of Big Data*, vol. 6, no. 29, 2019.
- [9] B. Bouchon-Meurier, G. Coletti, and R. R. Yager, *Modern information processing*. Elsevier Science, 2006.
- [10] Z. Yu, C. Chen, X. Zheng, W. Ding, and D. Chen, "Context-aware trust aided recommendation via Ontology and Gaussian mixture model in big data environment," in *2014 International Conference on Service Sciences*. IEEE, 2014, pp. 85–90.
- [11] H. Bi, H. Tang, G. Yang, H. Shu, and J.-L. Dillenseger, "Accurate image segmentation using Gaussian mixture model with saliency map," *Pattern Analysis and Applications*, vol. 21, pp. 869–878, 2018.
- [12] C.-A. Deledalle, S. Parameswaran, and T. Q. Nguyen, "Image denoising with generalized Gaussian mixture model patch priors," *SIAM Journal on Imaging Sciences*, vol. 11, no. 4, pp. 2568–2609, 2018.
- [13] K. Kalti and M. Mahjoub, "Image segmentation by Gaussian mixture models and modified FCM algorithm," *The International Arab Journal of Information Technology*, vol. 11, no. 1, pp. 11–18, 2014.
- [14] T. M. Nguyen and J. Wu, "Dirichlet Gaussian mixture model: Application to image segmentation," *Image and Vision Computing*, vol. 29, no. 12, pp. 818–828, 2011.
- [15] R. Farnoosh and B. Zarpak, "Image segmentation using Gaussian mixture model," *IUST International Journal of Engineering Science*, vol. 9, no. 1–2, pp. 29–32, 2008.
- [16] A. Alekseenko, T. Nguyen, and A. Wood, "A deterministic-stochastic method for computing the Boltzmann collision integral in O(MN) operations," *Kinetic & Related Models*, vol. 11, no. 5, pp. 1211–1234, 2018.
- [17] G. Chen, L. Chacon, and T. Nguyen, "An unsupervised machine-learning checkpoint-restart algorithm using Gaussian mixtures for particle-in-cell simulations," *submitted to Journal of Computational Physics*, arXiv:2007.12273, 2020.
- [18] R. Dupuis, M. V. Goldman, D. L. Newman, J. Amaya, and G. Lapenta, "Characterizing magnetic reconnection regions using Gaussian mixture models on particle velocity distributions," *The Astrophysical Journal*, vol. 889, no. 1, p. 22, 2020.
- [19] A. Barb, "Gaussian mixture models for semantic ranking in domain specific databases with application in radiology," *Central European Journal of Computer Science*, vol. 1, no. 3, pp. 266–279, 2011.
- [20] D. Reynolds, T. Quatieri, and R. Dunn, "Speaker verification using adapted Gaussian mixture models," *Digital Signal Processing*, vol. 10, no. 1–3, pp. 19–41, 2000.
- [21] B. Plataniotis, "Gaussian mixtures and their applications to signal processing," in *Advanced Signal Processing Handbook: Theory and Implementation for Radar, Sonar, and Medical Imaging Real Time Systems*, S. Stergiopoulos, Ed. Taylor & Francis Group, 2000, ch. 3.
- [22] D. Yu and L. Deng, "Gaussian mixture models," in *Automatic Speech Recognition*. Springer, 2015, pp. 13–21.
- [23] A. P. Dempster, N. M. Laird, and D. B. Rubin, "Maximum likelihood from incomplete data via the EM algorithm," *Journal of the royal statistical society. Series B (methodological)*, vol. 39, no. 1, pp. 1–38, 1977.
- [24] R. A. Redner and H. F. Walker, "Mixture densities, maximum likelihood and the EM algorithm," *SIAM review*, vol. 26, no. 2, pp. 195–239, 1984.
- [25] G. J. McLachlan and T. Krishnan, *The EM algorithm and extensions*. John Wiley & Sons, 2007, vol. 382.
- [26] G. J. McLachlan and S. Rathnayake, "On the number of components in a Gaussian mixture model," *Wiley Interdisciplinary Reviews: Data Mining and Knowledge Discovery*, vol. 4, no. 5, pp. 341–355, 2014.
- [27] M. A. Figueiredo and A. K. Jain, "Unsupervised selection and estimation of finite mixture models," in *Proceedings 15th International Conference on Pattern Recognition. ICPR-2000*, vol. 2. IEEE, 2000, pp. 87–90.
- [28] —, "Unsupervised learning of finite mixture models," *IEEE Transactions on Pattern Analysis and Machine Intelligence*, vol. 24, no. 3, pp. 381–396, 2002.
- [29] C. S. Wallace, *Statistical and inductive inference by minimum message length*. Berlin, Heidelberg: Springer-Verlag, 2005.
- [30] M. Hansen and B. Yu, "Model selection and the principle of minimum description length," *Journal of the American Statistical Association*, vol. 96, no. 454, pp. 746–774, 2001.
- [31] A. Corduneanu and C. M. Bishop, "Variational Bayesian model selection for mixture distributions," in *Artificial intelligence and statistics*, vol. 2001. Morgan Kaufmann Waltham, MA, 2001, pp. 27–34.
- [32] K. Lange, *Optimization*. Springer Science & Business Media, 2013.
- [33] X.-L. Meng and D. B. Rubin, "Maximum likelihood estimation via the ECM algorithm: A general framework," *Biometrika*, vol. 80, no. 2, pp. 267–278, 1993.
- [34] C. Liu and D. B. Rubin, "The ECME algorithm: a simple extension of EM and ECM with faster monotone convergence," *Biometrika*, vol. 81, no. 4, pp. 633–648, 1994.
- [35] J. A. Fessler and A. O. Hero, "Space-alternating generalized Expectation-Maximization algorithm," *IEEE Transactions on signal processing*, vol. 42, no. 10, pp. 2664–2677, 1994.
- [36] X.-L. Meng and D. Van Dyk, "The EM algorithm, an old folk song sung to a fast new tune," *Journal of the Royal Statistical Society: Series B (Statistical Methodology)*, vol. 59, no. 3, pp. 511–567, 1997.
- [37] C. Liu, D. B. Rubin, and Y. N. Wu, "Parameter expansion to accelerate EM: the PX-EM algorithm," *Biometrika*, vol. 85, no. 4, pp. 755–770, 1998.
- [38] G. Celeux, S. Chrétien, F. Forbes, and A. Mkhadri, "A component-wise EM algorithm for mixtures," *Journal of Computational and Graphical Statistics*, vol. 10, no. 4, pp. 697–712, 2001.
- [39] J. H. Wolfe, "Pattern clustering by multivariate mixture analysis," *Multivariate Behavioral Research*, vol. 5, no. 3, pp. 329–350, 1970.
- [40] T. A. Louis, "Finding the observed information matrix when using the EM algorithm," *Journal of the Royal Statistical Society: Series B (Methodological)*, vol. 44, no. 2, pp. 226–233, 1982.
- [41] R. Varadhan and C. Roland, "Simple and globally convergent methods for accelerating the convergence of any EM algorithm," *Scandinavian Journal of Statistics*, vol. 35, no. 2, pp. 335–353, 2008.
- [42] A. Berlinet and C. Roland, "Acceleration schemes with application to the EM algorithm," *Computational statistics & data analysis*, vol. 51, no. 8, pp. 3689–3702, 2007.
- [43] M. Jamshidian and R. I. Jennrich, "Conjugate gradient acceleration of the EM algorithm," *Journal of the American Statistical Association*, vol. 88, no. 421, pp. 221–228, 1993.
- [44] R. Salakhutdinov, S. T. Roweis, and Z. Ghahramani, "Optimization with EM and expectation-conjugate-gradient," in *Proceedings of the 20th International Conference on Machine Learning (ICML-03)*, 2003, pp. 672–679.

- [45] Y. He and C. Liu, "The dynamic "expectation–conditional maximization either" algorithm," *Journal of the Royal Statistical Society: Series B (Statistical Methodology)*, vol. 74, no. 2, pp. 313–336, 2012.
- [46] K. Lange, "A quasi-newtonian acceleration of the EM algorithm," *Statistica Sinica*, vol. 5, pp. 1–18, 1995.
- [47] M. Jamshidian and R. I. Jennrich, "Acceleration of the EM algorithm by using quasi-Newton methods," *Journal of the Royal Statistical Society: Series B (Statistical Methodology)*, vol. 59, no. 3, pp. 569–587, 1997.
- [48] N. Henderson and R. Varadhan, "Damped Anderson acceleration with restarts and monotonicity control for accelerating EM and EM-like algorithms," *Journal of Computational and Graphical Statistics*, vol. 28, no. 4, pp. 834–846, 2019.
- [49] H. Zhou, D. Alexander, and K. Lange, "A quasi-Newton acceleration for high-dimensional optimization algorithms," *Statistics and computing*, vol. 21, no. 2, pp. 261–273, 2011.
- [50] I. Meilijson, "A fast improvement to the EM algorithm on its own terms," *Journal of the Royal Statistical Society: Series B (Methodological)*, vol. 51, no. 1, pp. 127–138, 1989.
- [51] K. Lange, "A gradient algorithm locally equivalent to the EM algorithm," *Journal of the Royal Statistical Society: Series B (Methodological)*, vol. 57, no. 2, pp. 425–437, 1995.
- [52] D. G. Anderson, "Iterative procedures for nonlinear integral equations," *J. Assoc. Comput. Mach.*, vol. 12, pp. 547–560, 1965.
- [53] H.-r. Fang and Y. Saad, "Two classes of multisection methods for nonlinear acceleration," *Numerical Linear Algebra with Applications*, vol. 16, no. 3, pp. 197–221, 2009.
- [54] H. F. Walker and P. Ni, "Anderson acceleration for fixed-point iterations," *SIAM Journal on Numerical Analysis*, vol. 49, no. 4, pp. 1715–1735, 2011.
- [55] J. H. Plasse, "The EM algorithm in multivariate Gaussian mixture models using Anderson acceleration," Master's thesis, Worcester Polytechnic Institute, April 2013.
- [56] R. Tibshirani, G. Walther, and T. Hastie, "Estimating the number of clusters in a data set via the gap statistic," *Journal of Royal Statistical Society: Series B (Statistical Methodology)*, vol. 63, no. 2, pp. 411–423, 2001.
- [57] B. S. Everitt, "Finite mixture distributions," *Wiley StatsRef: Statistics Reference Online*, 2014.
- [58] V. Hasselblad, "Estimation of parameters for a mixture of normal distributions," *Technometrics*, vol. 8, no. 3, pp. 431–444, 1966.
- [59] J. Behboodiani, "On a mixture of normal distributions," *Biometrika*, vol. 34, no. 57 Part 1, pp. 215–217, 1970.
- [60] D. J. C. MacKay, *Information theory, inference and learning algorithms*. USA: Cambridge University Press, 2003.
- [61] J. Rousseau and K. Mengersen, "Asymptotic behaviour of the posterior distribution in overfitted mixture models," *Journal of the Royal Statistical Society: Series B (Statistical Methodology)*, vol. 73, no. 5, pp. 689–710, 2011.
- [62] Y. Raykov, A. Boukouvalas, F. Baig, and M. Little, "What to do when K-means clustering fails: A simple yet principled alternative algorithm," *PLoS ONE*, vol. 11, no. 9, 2016.
- [63] C. Darken and J. Moody, "Fast adaptive K-means clustering: some empirical results," in *1990 IJCNN International Joint Conference on Neural Networks*, vol. 2. IEEE, 1990, pp. 233–238.
- [64] Scikit-Learn Library, *Selecting the number of clusters with silhouette analysis on K-Means clustering*, 2007–2020. [Online]. Available: https://scikit-learn.org/stable/auto_examples/cluster/plot_kmeans_silhouette_analysis.html
- [65] P. J. Rousseeuw, "Silhouettes: a graphical aid to the interpretation and validation of cluster analysis," *Journal of Computational and Applied Mathematics*, vol. 20, pp. 53–65, 1987.
- [66] S. Nanjundan, S. Sankaran, C. R. Arjun, and P. Anand, "Identifying the number of clusters for K-means: A hypersphere density based approach," in *International Conference on Computers, Communication and Signal Processing - 2019*, 2019.
- [67] W. Xiang, A. Karfoul, C. Yang, H. Shu, and R. L. B. Jeannès, "An exact line search scheme to accelerate the EM algorithm: Application to Gaussian mixture models identification," *Journal of Computational Science*, vol. 41, p. 101073, 2020.
- [68] N. N. Carlson and K. Miller, "Design and application of a gradient-weighted moving finite element code i: In one dimension," *SIAM J. Sci. Comput.*, vol. 19, no. 3, pp. 728–765, 1998.
- [69] H. An, X. Jia, and H. F. Walker, "Anderson acceleration and application to the three-temperature energy equations," *J. Comput. Phys.*, vol. 347, no. 15, pp. 1–19, 2017.
- [70] X. Chen and C. Kelley, "Convergence of the EDIIS algorithm for nonlinear equations," *SIAM Journal on Scientific Computing*, vol. 41, no. 1, pp. A365–A379, 2019.
- [71] P. R. Pratapa and P. Suryanarayana, "Restarted Pulay mixing for efficient and robust acceleration of fixed-point iterations," *Chemical Physical Letters*, vol. 635, pp. 69–74, 2015.
- [72] D. Arthur and S. Vassilvitskii, "K-means++: the advantages of careful seeding," in *In Proceedings of the 18th Annual ACM-SIAM Symposium on Discrete Algorithms*, 2007, pp. 1027–1035.
- [73] R. A. Horn and C. R. Johnson, *Matrix analysis*. Cambridge university press, 2012.
- [74] C. K. Birdsall and A. B. Langdon, *Plasma physics via computer simulation*. CRC press, 2004.
- [75] E. S. Weibel, "Spontaneously growing transverse waves in a plasma due to an anisotropic velocity distribution," *Physical Review Letters*, vol. 2, no. 3, p. 83, 1959.
- [76] K. B. Petersen and M. S. Pedersen, "The matrix cookbook," nov 2012, version 20121115. [Online]. Available: <http://www2.compute.dtu.dk/pubdb/pubs/3274-full.html>